

ACHIEVING ACCELERATION DESPITE VERY NOISY GRADIENTS

KANAN GUPTA, JONATHAN SIEGEL, AND STEPHAN WOJTOWYTSCH

ABSTRACT. We present a novel momentum-based first order optimization method (AGNES) which provably achieves acceleration for convex minimization, even if the stochastic noise in the gradient estimates is many orders of magnitude larger than the gradient itself. Here we model the noise as having a variance which is proportional to the magnitude of the underlying gradient. We argue, based upon empirical evidence, that this is appropriate for mini-batch gradients in overparameterized deep learning. Furthermore, we demonstrate that the method achieves competitive performance in the training of CNNs on MNIST and CIFAR-10.

1. INTRODUCTION

Much of the computational effort in modern deep learning is spent on the parameter optimization (or training) of neural networks. Almost all state of the art training algorithms are stochastic first order methods, i.e. methods based on stochastic estimates for the parameter gradient of a neural network. While some very popular methods employ coordinate-wise non-Euclidean geometry (such as Adam, RMSprop, and possibly most evidently signSGD), the underlying intuition derives from simple Euclidean models: The gradient flow and Newton’s second law (or the ‘heavy ball ODE’)

$$\dot{x} = -\nabla f(x) \quad \text{and} \quad \ddot{x} = -\mu\dot{x} - \nabla f(x)$$

respectively. The gradient flow can be thought of as inspired by a hiker on a foggy day, carefully weighing their steps and walking in the most promising direction of steepest descent, whereas the heavy ball ODE models a particle of unit mass barrelling down a mountainside under the influence of the energy potential f and Stokes’ friction with strength μ . While the gradient flow follows a locally optimal trajectory, the heavy ball retains a memory of past slopes along its trajectory via the second order time derivative. In ‘nice’ objective landscapes, this global information can be leveraged to attain much faster convergence.

Time-discretizations of the gradient flow ODE (gradient descent) and the heavy ball ODE (gradient descent with momentum, Nesterov’s accelerated gradient method) are fundamental optimization methods for deep learning. While stochastic gradient descent has been analyzed in detail, momentum methods have resisted generalization to the stochastic setting to a larger degree. Despite a lack of theoretical guarantees, using momentum-based optimizers with stochastic gradients is necessary for the training of neural networks in reasonable time. Even for a small neural network with less than 100,000 parameters, the noise in the gradient estimates can easily be five orders of magnitude larger than the parameter gradient itself.

We address this gap between deep learning theory and practice by presenting the novel Nesterov type method AGNES, which provably achieves acceleration in the stochastic case. AGNES (Accelerated Gradient descent with Noisy EStimators) is a generalization of the SGD optimizer implemented in Pytorch or Tensorflow (with momentum). It requires only one additional vector addition compared to the simplest version of the current algorithm.

In more technical terms, we demonstrate that AGNES achieves the $O(1/n^2)$ decay rate in the stochastic setting, which is also optimal in deterministic first order optimization for convex objectives.

2020 *Mathematics Subject Classification.* 68T07, 60J20, 65C99.

Key words and phrases. Deep learning, accelerated gradient descent, stochastic optimization, stochastic acceleration, convex optimization.

The noise in our analysis satisfies a multiplicative type scaling assumption, which we demonstrate closely captures the scaling in minibatch gradient estimators. While the decay rate is unaffected by the stochasticity in the gradient estimates, the constants scale proportionally to the square of the noise intensity in a precise fashion.

This article is organized as follows. In the remainder of the introduction, we review previous work on stochastic optimization and accelerated gradient descent algorithms. In Section 2, we discuss the theoretical context of our work in overparametrized deep learning and modelling aspects for the stochastic noise. The novel descent algorithm is presented in Section 3, along with our main convergence results. Numerical evidence for its efficacy in a deep learning application is provided in Section 4. In the appendix, we present the proofs of our main results, along with simulations in the context of stochastic convex minimization which match our theoretical guarantees.

1.1. Previous work. There is a long history of iterative methods in numerical linear algebra which use information gained along the trajectory to accelerate convergence compared to methods using purely local information. One such example is the conjugate gradient (CG) algorithm introduced by Hestenes et al. [1952] for the solution of linear systems with positive definite matrices, a problem which is equivalent to the minimization of quadratic objective functions. Based upon these ideas, Polyak [1964] introduced the Heavy-ball method, which achieves accelerated convergence locally for C^2 functions near a local minimizer with positive definite Hessian. Developing these ideas further, Nesterov [1983] devised a celebrated method which achieves accelerated convergence *globally* for convex objectives.

Nesterov's accelerated method has subsequently been extensively studied and generalized by many authors. For instance, Beck and Teboulle [2009] demonstrate how to accelerate proximal gradient methods, which results in the celebrated FISTA algorithm in image processing, which was further studied by Beck and Teboulle [2009], Chambolle and Dossal [2015], Kim and Fessler [2018].

Another important line of research is to gain an understanding of how accelerated methods work, which can be used to design novel accelerated methods in other contexts. In this direction, Bubeck et al. [2015] gives a geometric derivation of accelerated methods and Su et al. [2014]'s seminal analysis characterized accelerated methods in terms of ordinary differential equations. The differential equation point of view has subsequently been pushed further by many authors, including Zhang et al. [2018], Wilson et al. [2021], Attouch et al. [2022], Siegel [2019], Aujol et al. [2022b,a], Dambrine et al. [2022]. This line of research has resulted in the design of novel accelerated methods based upon discretizing dynamical systems.

Optimization algorithms where gradients are only estimated by a stochastic oracle were first introduced in a seminal article by Robbins and Monro [1951]. Early studies were motivated by noise in statistical mechanics, which corresponds to random particle oscillations at small positive temperature. Such noise is homogeneous over the state space, often isotropic, and 'additive' in nature. It can be modelled after the gradient oracle $g_n = \nabla f(x_n) + \sigma N_n$, where the random variables N_n are independent with zero mean and unit variance. More generally, the governing assumption is that the gradient oracles satisfy a variance bound $\mathbb{E}[\|g - \nabla f(x)\|^2] \leq \sigma^2$. Subsequent studies by many authors, including Mertikopoulos et al. [2020], Dereich and Kassing [2021], Patel and Zhang [2021], Patel and Berahas [2022] considered more general regularity assumptions on the objective function f and more general moment bounds on the gradient oracle g .

Stochastic gradient algorithms have received renewed attention more recently in the context of deep learning. A more detailed introduction is given e.g. by LeCun et al. [2015], Bottou et al. [2018]. A continuous time model was derived by Li et al. [2017], and various fine properties such as the minimum selection mechanism (or 'implicit bias') and the escape from local minimizers were studied by Wu et al. [2018], Liu et al. [2020], Simsekli et al. [2020], Ziyin et al. [2021], Mori et al. [2021], Pesme et al. [2021], Andriushchenko et al. [2023].

In deep learning, the additive noise assumption is less well motivated, as the noise is of low rank and degenerates on the set of global minimizers. Various non-standard noise models have been considered in a discrete time setting by Stich [2019], Stich and Karimireddy [2022], Bassily et al. [2018], Gower

et al. [2019], Damian et al. [2021], Wojtowytsch [2021b], Zhou et al. [2020] and the continuous time limit by Wojtowytsch [2021a], Zhou et al. [2020], Li et al. [2022]. These include noise assumptions for degenerate noise due to Bassily et al. [2018], Damian et al. [2021], Wojtowytsch [2021b,a], low rank noise studied by Damian et al. [2021], Li et al. [2022] and noise with heavy tails explored by Zhou et al. [2020].

Ziyin et al. [2022] sketch a particularly antagonistic combination of noise and loss landscape which leads to SGD trajectories which converge to local *maxima*. Such examples illustrate the importance of noise and landscape modelling.

Several advanced stochastic optimizers built around adaptive learning rates, in part utilizing non-Euclidean coordinatewise descent schemes, have been studied under additive noise models for non-convex objective functions by Bernstein et al. [2018], Ward et al. [2019], Safaryan and Richtárik [2021], Défossez et al. [2022].

Previous works on accelerated stochastic gradient algorithms fall into two categories: Works on specific problems in machine learning with minibatch gradient estimates and works on accelerated gradient descent methods with additive noise. In the second setting, Laborde and Oberman [2020] give a great review of existing results and improve the rate of convergence in a general setting. The deterministic rate of $O(1/n^2)$ is unattainable under these general assumptions.

Accelerating the convergence of stochastic optimization methods is a subtle effort. Kidambi et al. [2018] prove that there are situations in which it is impossible for any first order oracle method to improve upon SGD due to information-theoretic lower bounds. More generally, lower bounds in the stochastic first order oracle (SFO) model were presented by Agarwal et al. [2009]. A partial improvement on the state of the art is given by Jain et al. [2018], who present an ASGD method motivated by a particular low-dimensional and strongly convex problem.

Most closely to our current work, Bollapragada et al. [2022] study an accelerated gradient method for the optimization of a strongly convex quadratic objective function with minibatch noise. We crucially improve on their result in two ways:

- (1) We allow general convex objective functions rather than limiting ourselves to quadratics.
- (2) We are able to handle arbitrary noise intensities with a batch size of 1, rather than requiring sufficiently large batches to ‘tame’ the stochastic oscillations.

As a distinction, we note that our analysis is set in convex optimization rather than the strongly convex case. The results are therefore not comparable in a precise sense.

2. BACKGROUND

2.1. Minibatch noise in overparametrized learning. In supervised learning applications, the learning task often corresponds to minimizing a risk or loss function $\mathcal{R}(w) = \frac{1}{n} \sum_{i=1}^n \ell(h(w, x_i), y_i) =: \frac{1}{n} \sum_{i=1}^n \ell_i(w)$, where

$$h : \mathbb{R}^m \times \mathbb{R}^d \rightarrow \mathbb{R}^k, \quad (w, x) \mapsto h(w, x), \quad \text{and} \quad \ell : \mathbb{R}^k \times \mathbb{R}^k \rightarrow [0, \infty)$$

are a parametrized function of weights w and data x and a loss function measuring compliance between $h(w, x_i)$ and y_i respectively.¹ When working with neural networks, the number of network parameters m usually vastly exceeds the number of data points n . Chizat and Bach [2018], Du et al. [2018b] show that working in the overparametrized regime simplifies the optimization process and Belkin et al. [2019, 2020] illustrate that it facilitates generalization to previously unseen data. Fitting n constraints with m parameters typically leads to the existence of an $m - n$ -dimensional solution submanifold \mathcal{M} of the parameter space \mathbb{R}^m such that all given labels y_i are fit exactly by $h(w, \cdot)$ at the data points x_i , i.e. $\mathcal{R} \equiv 0$ on \mathcal{M} . This intuition was made precise by Cooper [2019] using the regular value theorem and the Morse-Sard theorem.

¹ Both ℓ and \mathcal{R} are commonly called a ‘loss function’ in the literature. To distinguish between the two, we will borrow the terminology of statistics and refer to \mathcal{R} as the risk functional and ℓ as the loss function. The notation L , which is often used in place of \mathcal{R} , is reserved for the Lipschitz constant in this work.

Since the number m of model parameters is large, often on the order of millions and more recently billions, many sophisticated tools from optimization theory cannot be applied in deep learning. Despite promising work on quasi-Newton methods due to Berahas et al. [2016], Moritz et al. [2016], Bollapragada et al. [2018], Chang et al. [2019] and employed e.g. by Lou et al. [2021], simple first order methods, which only require first derivatives of the risk function, remain the state of the art.

If the number of data points is large, it is even computationally expensive to calculate the gradient $\nabla\mathcal{R}(w) = \frac{1}{n} \sum_{i=1}^n \sum_{j=1}^k \nabla\ell_i$ of the risk function \mathcal{R} exactly. A common workaround for this issue is to work with stochastic gradient estimates

$$g = \frac{1}{n_b} \sum_{i \in I_b} \nabla\ell_i(w) = \frac{1}{n_b} \sum_{i \in I_b} \sum_{j=1}^k (\partial_{h_j} \ell)(h(w, x_i), y_i) \nabla_w h_j(w, x_i),$$

where $I_b \subseteq \{1, \dots, n\}$ is a subsampled collection of n_b data points (a batch or minibatch). Minibatch stochastic gradient estimates are very different from the stochasticity we encounter e.g. in statistical mechanics:

- (1) The covariance matrix $\Sigma = \frac{1}{n} \sum_{i=1}^n (\nabla\ell_i - \nabla\mathcal{R}) \otimes (\nabla\ell_i - \nabla\mathcal{R})$ of the gradient estimators $\nabla\ell_i$ has rank $n \ll m$, i.e. the noise has much lower rank than the dimension of the parameter space.
- (2) Assume specifically that ℓ is a loss function which satisfies $\ell(y, y) = 0$ for all $y \in \mathbb{R}^k$, such as the popular ℓ^2 - or mean squared error (MSE) loss function $\ell(f, y) = \|f - y\|^2$ or a Huber-type loss. Then $\nabla\ell_i(w) = 0$ for all $i \in \{1, \dots, n\}$ and all $w \in \mathcal{M} = \mathcal{R}^{-1}(0)$.

In particular, the stochastic noise vanishes on the interpolating manifold \mathcal{M} in the overparametrized regime.

The following Lemma makes the second observation precise in the overparameterized regime and bounds the stochasticity of mini-batch estimates more generally.

Lemma 1 (Noise intensity). *Assume that $\ell(h, y) = \|h - y\|^2$ and $f : \mathbb{R}^m \rightarrow \mathbb{R}^k$ satisfies*

$$\|\nabla_w h(w, x_i)\|^2 \leq C(1 + \|w\|)^p \quad \forall w \in \mathbb{R}^m, i = 1, \dots, n$$

for some $C, p > 0$. Then

$$\frac{1}{n} \sum_{i=1}^n \|\nabla\ell_i - \nabla\mathcal{R}\|^2 \leq C^2 (1 + \|w\|)^{2p} \mathcal{R}(w) \quad \forall w \in \mathbb{R}^m.$$

The proof of Lemma 1 can be found in Appendix C. It is a modification of [Wojtowytsch, 2021b, Lemma 2.14] for function models which are not globally Lipschitz in the weights w .

Lemma 1 describes the variance of a gradient estimator which uses a randomly selected index $i \in \{1, \dots, n\}$ and the associated gradient $\nabla\ell_i$ is used to approximate $\nabla\mathcal{R}$. If a batch I_b of n_b indices is selected randomly with repetition, then the variance of the gradient estimators scales in the usual way:

$$(2.1) \quad \mathbb{E}_{|I_b|=n_b} \left[\left\| \frac{1}{n_b} \sum_{i \in I_b} \nabla\ell_i - \nabla\mathcal{R} \right\|^2 \right] \leq \frac{C^2(1 + \|w\|)^{2p}}{n_b} \mathcal{R}(w).$$

If a random batch I_b is selected *without* repetition, the variance is smaller – in the extreme case $n_b = n$, we compute with exact gradients. As usual, if the batch size is much smaller than the size of the data set, the heuristic variance scaling $\sigma^2 \rightarrow \sigma^2/n_b$ is approximately accurate.

Another difference between minibatch optimization in theory and practice arises as gradient estimators are correlated between time-steps. Current practice in deep learning employs a random pass version of SGD, where the entire data set is iterated through in random order for gradient estimates before reusing the same data point. In theoretical analyses, we are restricted to random choice SGD, where a batch of data is selected randomly at every step independently of the batches in previous steps.

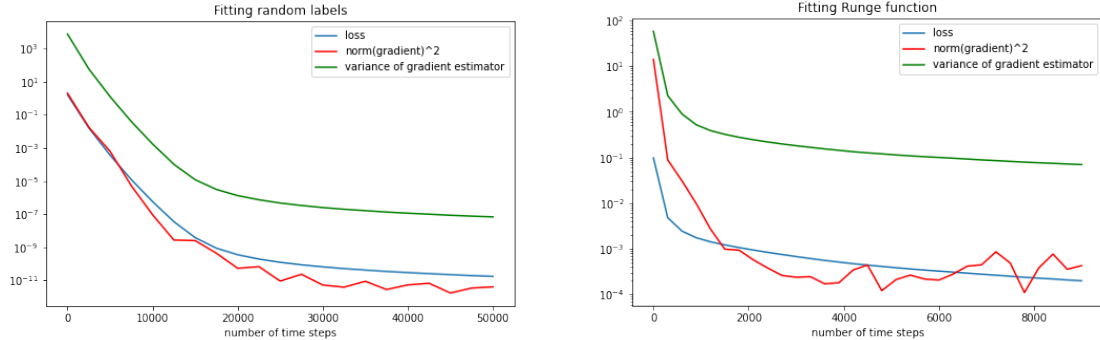


FIGURE 1. **Left:** A ReLU network with four hidden layers of width 250 is trained by SGD to fit random labels y_i (drawn from a 2-dimensional standard Gaussian) at 1,000 random data points x_i (drawn from a 500-dimensional standard Gaussian). The variance σ^2 of the gradient estimators is $\sim 10^5$ times larger than the loss function and $\sim 10^6$ times larger than the parameter gradient. This relationship is stable over approximately ten orders of magnitude. **Middle:** A ReLU network with two hidden layers of width 50 is trained by SGD to fit the Runge objective function $1/(1+x^2)$ on equispaced data samples in the interval $[-8, 8]$, which is challenging for polynomial interpolation. Also here, the variance in the gradient estimates is proportional to both the loss function and the magnitude of the gradient. **Right:** Approximation of the Runge function by ReLU networks.

Heuristically, we can consider the procedures as sufficiently similar for large data sets and simply note that the true stochasticity is likely even lower in practice than Lemma 1 suggests.

A numerical illustration of the scaling given by Lemma 1 is given in Figure 1, where we also observe that the intensity of the noise in the gradient estimators scales roughly linearly with the magnitude of the true parameter gradients. Due to the high dimension of the parameter space, we are unable to explore the relationship at all points, and relate the oscillation of the gradient estimators along an optimization trajectory instead. To be able to quantify the gradient noise exactly, we choose relatively small models and data sets.

The type of stochasticity where the noise-to-signal ratio is $\Theta(1)$ is often referred to as ‘multiplicative noise’, as it resembles the noise generated by estimates of the form $g = (1 + \sigma N)\nabla\mathcal{R}$, where N is a random variable with mean zero and unit variance. We make a multiplicative noise assumption in this analysis rather than the more subtle scaling assumption of (2.1). In a setting where the objective function has a Lipschitz-continuous gradient and satisfies a PL condition (see e.g. Karimi et al. [2016]), both assumptions are equivalent.

For the sake of generality and ease of notation, we assume more generally that we are minimizing a general function $f : \mathbb{R}^m \rightarrow \mathbb{R}$ and have access to a random function g such that at a fixed point x we obtain

$$\mathbb{E}[g(x)] = \nabla f(x), \quad \mathbb{E}[\|g(x) - \nabla f(x)\|^2] \leq \sigma^2 \|\nabla f(x)\|^2.$$

This setting includes minibatch gradient estimators as well as using single data points for estimation, at least while the optimization algorithm does not leave a bounded domain inside of which we can consider the proxy σ for $C(1 + \|w\|)^p$ to be bounded.

2.2. On the (non-)convexity of loss landscapes in deep learning. Optimization tasks in deep learning are notoriously non-convex, and Safran and Shamir [2018] prove that many local minimizers exist in the underparametrized regime. We illustrate that barriers to convexity exist also in the overparametrized regime and sketch the limitations of analyses using convexity in Appendix D.

Despite the non-convexity, loss functions have many beneficial properties in the overparametrized regime. For example, any point in the MSE-loss landscape of an overparametrized neural network with a single hidden layer is connected to a global minimizer by a path of non-increasing loss as shown by Nguyen et al. [2019] and [Foucart, 2022, Section 27.2]. In particular, all strict local minimizers are global minimizers. The fact that loss landscapes appear to be ‘nice’ but non-convex has lead to studies of stochastic gradient descent in neural network optimization under less geometrically restrictive assumptions, such as the Polyak-Łojasiewicz (or PL) condition, by Karimi et al. [2016], Wojtowytsh [2021b]. Despite recent progress in relaxing convexity conditions by Aujol et al. [2022b,a], accelerated gradient descent requires stronger global properties of the loss landscape than mere gradient descent, as it aims to average global geometric information (or at least, information along its trajectory).

Convex optimization captures certain limiting regimes very well. For heavily overparametrized neural networks, the optimization process is close to that of a linear method (the ‘neural tangent kernel’ or NTK), which is derived from linearization at the random initialization as explored by Jacot et al. [2018b], Du et al. [2018b,a], Jacot et al. [2018a], E et al. [2020], Arora et al. [2019], Jentzen and Kröger [2021] and many others. The kernel depends on the law of the initialization, but not the realization. Since the NTK is linear in its parameters, this optimization problem is even strongly convex, although with a generally very small strong convexity parameter.

Given that realistic risk functionals in deep learning share many favorable properties of convex functions, we believe convex optimization to be an insightful toy model for optimization in deep learning and a suitable test setting for improved algorithms. Still, we acknowledge the fundamental limitations of such analyses.

3. ALGORITHM AND CONVERGENCE GUARANTEES

3.1. Descent algorithm. Let f be an objective function and x_0 an initialization such that $\mathbb{E}[f(x_0) + \|x_0\|^2] < \infty$. We propose the following scheme for Accelerated Gradient descent with Noisy EStimators (AGNES):

- (1) Select hyperparameters $\alpha, \eta, \gamma > 0$ and a sequence of decay factors $\rho_n \in (0, 1)$.
- (2) Set $v_0 = 0$.
- (3) Use the following update rules to generate a sequence of locations and velocities (x_n, v_n) :

$$x'_n = x_n + \alpha v_n, \quad x_{n+1} = x'_n - \eta g_n, \quad v_{n+1} = \rho_n(v_n - \gamma g_n).$$

Here g_n is a gradient estimator for f at the auxiliary point x'_n , i.e. $\mathbb{E}[g_n | \mathcal{F}_n] = \nabla f(x'_n)$.

We compare AGNES to versions of the SGD optimizer with momentum in Appendix B and prove that it generalizes all currently implemented versions. The parameters α, γ are redundant in the sense that one of them could be eliminated from the scheme. In the numerical implementation, we therefore set $\gamma = 1$ as default choice.

Lemma 2. *Let $\rho \in (0, 1)$ and $\eta > 0$ parameters. Assume that α, γ and $\tilde{\alpha}, \tilde{\gamma}$ are parameters such that $\tilde{\alpha}\tilde{\gamma} = \alpha\gamma$. Consider the sequences $(\tilde{x}_n, \tilde{x}'_n, \tilde{v}_n)$ and (x_n, x'_n, v_n) generated by the time stepping scheme with parameters $(\rho, \eta, \tilde{\alpha}, \tilde{\gamma})$ and $(\rho, \eta, \alpha, \gamma)$ respectively. If $x_0 = \tilde{x}_0$ and $\alpha v_0 = \tilde{\alpha} \tilde{v}_0$, then $x_n = \tilde{x}_n$, $x'_n = \tilde{x}'_n$ and $\tilde{\alpha} \tilde{v}_n = \alpha v_n$ for all $n \in \mathbb{N}$.*

The proof of Lemma 2 is given in Appendix E. We give a set of suggested hyperparameters that we found to work well for machine learning in the schematic representation in Algorithm 3.1. For compatibility with the typical workflow in PyTorch where gradient estimates are computed *outside* the optimizer, the numerical scheme returns the sequence x'_{n+1} rather than x_{n+1} , as we require the gradient estimate at this point. Alternatively, an estimate for $\nabla f(x_n)$ could be used, although we have no theoretic guarantees in this case. We maintain that this departure from the theoretical procedure for applications in deep learning is well justified by its empirical performance.

Algorithm 1 Accelerated Gradient descent with Noisy EStimators (AGNES)

Input: f (objective function), x_0 (initial point), $\alpha = 10^{-3}$ (learning rate), $\eta = 5 \cdot 10^{-3}$ (correction step), $\rho = 0.99$ (friction), N (number of iterations)

```

 $n \leftarrow 0$ 
 $v_0 \leftarrow 0$ 
while  $n < N$  do
     $n \leftarrow n + 1$ 
     $g_{n-1} \leftarrow \nabla_x f(x_{n-1})$  ▷ (mini-batch/stochastic gradient at  $x_{n-1}$ )
     $x_n \leftarrow x_{n-1} + \alpha v_{n-1} - \eta g_{n-1}$ 
     $v_n \leftarrow \rho(v_{n-1} - g_{n-1})$ 
end while
return  $x_n$ 

```

3.2. Continuous time interpretation. For better interpretability, we consider the continuous time limit of the AGNES algorithm. Assume that $\eta = c_1 h$, $\alpha = \gamma = c_2 h$ and $\rho = 1 - c_3 h$ for some constants $c_1, c_2, c_3 \geq 0$ and a small parameter h . In the deterministic case $g_n = \nabla f(x'_n)$, we have

$$\begin{pmatrix} x_{n+1} \\ v_{n+1} \end{pmatrix} = \begin{pmatrix} x_n \\ v_n \end{pmatrix} + h \begin{pmatrix} c_2 v_n - c_1 \nabla f(x'_n) \\ -c_3 v_n - (1 - c_3 h) c_2 \nabla f(x'_n) \end{pmatrix} = \begin{pmatrix} x_n \\ v_n \end{pmatrix} + h \begin{pmatrix} c_2 v_n - c_1 \nabla f(x_n) \\ -c_3 v_n - c_2 \nabla f(x_n) \end{pmatrix} + O(h^2)$$

which is a time-stepping scheme for the coupled ODE system

$$\begin{pmatrix} \dot{x} \\ \dot{v} \end{pmatrix} = \begin{pmatrix} c_2 v - c_1 \nabla f(x) \\ -c_3 v - c_2 \nabla f(x) \end{pmatrix}.$$

Differentiating the first equation and using the system ODEs to subsequently eliminate v from the expression, we observe that

$$\begin{aligned} \ddot{x} &= c_2 \dot{v} - c_1 D^2 f(x) \dot{x} \\ &= c_2 (-c_3 v - c_2 \nabla f(x)) - c_1 D^2 f(x) \dot{x} \\ &= -c_3 (\dot{x} + c_1 \nabla f(x)) - c_2^2 \nabla f(x) - c_1 D^2 f(x) \dot{x} \\ &= - (c_3 I + c_1 D^2 f(x)) \dot{x} - (c_1 c_3 + c_2^2) \nabla f(x). \end{aligned}$$

Observe that c_2 only enters quadratically, as only the product of α and γ influences the algorithm even in continuous time. The AGNES scheme is only a discretization of the heavy ball ODE

$$\ddot{x} = -\mu \dot{x} - \nabla f(x)$$

if $c_1 = 0$. A scaling where $c_1 > 0$ introduces an additional adaptive friction tailored to the geometry of the objective function f . In Theorem 4 below, we consider $c_1 h = \eta = 2 \alpha \gamma = 2 c_2^2 h^2$, so $c_1 = 2 c_2^2 h$. Hence asymptotically, we recover the heavy ball dynamics in this parameter regime.

3.3. Assumptions. In the remainder of this article, we consider the task of minimizing an objective function $f : \mathbb{R}^m \rightarrow \mathbb{R}$ using stochastic gradient estimates g . We assume that f , g and the initial condition x_0 have the following properties:

- (1) $v_0 \equiv 0$ and $x_0 = x'_0$ is a (potentially random) initial condition such that $\mathbb{E}[f(x_0) + \|x_0\|^2] < \infty$.
- (2) f is L -smooth, i.e. ∇f is L -Lipschitz continuous with respect to the Euclidean norm.
- (3) (g_n) is a sequence of gradient estimators for f satisfying two properties:
 - (a) $\mathbb{E}[g_n | \mathcal{F}_n] = \nabla f(x'_n)$ (unbiased gradient oracle)
 - (b) $\mathbb{E}[\|g_n - \nabla f(x'_n)\|^2 | \mathcal{F}_n] \leq \sigma^2 \|\nabla f(x'_n)\|^2$ (multiplicative noise scaling).

Here $\mathbb{E}[\cdot | \mathcal{F}_n]$ denotes the conditional expectation with respect to the σ -algebra $\mathcal{F}_n = \sigma(\{x_k, x'_k, v_k, : 0 \leq k \leq n\})$ generated by the sequence of random variables (x_n, x'_n, v_n) derived from the descent algorithm as described in Section 3.1.

Conditional expectations are a technical tool to account for inherent randomness and additional randomness. For example, if x_n is a random variable, then $\nabla f(x_n)$ is a stochastic gradient estimator, but it is perfectly accurate once x_n is known. This ‘inherent randomness’ is captured by the conditional expectations. A more detailed review can be found in Appendix F.

An easy example for suitable gradient estimators is that of random functions $g : \mathbb{R}^m \times \Omega \rightarrow \mathbb{R}^m$ such that

$$\mathbb{E}_\omega g(x, \omega) = \nabla f(x) \quad \forall x \in \mathbb{R}^m$$

and considering the sequence $g_n = g(x'_n, \omega_n)$ where the random elements ω_n are drawn from Ω independently. More crucially, these assumptions apply to ‘random selection’ minibatch gradient descent for deep learning.

3.4. Convergence guarantees. Gradient descent with momentum is not particularly adapted to non-convex optimization – without stronger control, momentum on the contrary may lead to avoidance of critical points which are not local minimizers. We note that the algorithm may perform worse than stochastic gradient descent, but that for suitable parameters, the performance is comparable to that of SGD within a constant factor.

Theorem 3 (Non-convex case). *Assume that f satisfies the assumptions laid out in Section 3.3. Let $\eta, \alpha, \gamma, \rho$ be such that*

$$\eta \leq \frac{1}{L(1 + \sigma^2)}, \quad \alpha\gamma < \frac{\eta}{1 + \sigma^2}, \quad (L\alpha\gamma + 1)\rho^2 \leq 1.$$

Then

$$\min_{1 \leq i \leq n} \mathbb{E}[\|\nabla f(x_i)\|^2] \leq \frac{2 \mathbb{E} \left[f(x_1) - \inf f + \frac{1}{\alpha\gamma\rho^2} \|v_1\|^2 \right]}{n(\eta - \alpha\gamma(1 + \sigma^2))}.$$

The proof of Theorem 3 is given in Appendix G, along with a more detailed exploration of the choice of parameters. The descent algorithm shows its strength in the convex case rather than a generic non-convex situation.

Theorem 4 (Convex case). *Assume that, in addition to the assumptions laid out in Section 3.3, the objective function f is convex and that x^* is a point such that $f(x^*) = \inf_{x \in \mathbb{R}^m} f(x)$. Assume that α, η, γ are parameters such that*

$$\eta = \frac{1}{L(1 + \sigma^2)}, \quad \gamma\alpha = \frac{\eta}{2(1 + \sigma^2)}, \quad n_0 \geq \sqrt{(2\sigma)^4 + 24\sigma^2 + 10} - 2, \quad \rho_n = \frac{n + n_0}{n + n_0 + 3}$$

and $\rho_n = \frac{n + n_0}{n + n_0 + 3}$. Then

$$\mathbb{E}[f(x_n) - f(x^*)] \leq \frac{\mathbb{E}[(n_0\gamma\alpha + 2\eta)n_0(f(x_0) - \inf f) + 2\|x_0 - x^*\|^2]}{\gamma\alpha(n + n_0)^2}.$$

Furthermore $f(x_n) \rightarrow \inf f$ with probability 1.

The proof of Theorem 4 is given in Appendix H. We note that the benefit of the accelerated gradient scheme is an improvement from a decay rate of $1/n$ to the rate $1/n^2$, which is optimal under the given assumptions even in the deterministic case. While the noise can be many orders of magnitude larger than the quantity we want to estimate, it only affects the constants in the convergence, but not the rate.

Remark 5 (batch size). We can compare two versions of AGNES:

- (1) After computing a gradient, we take a step with the optimizer.
- (2) We obtain n_b gradient estimates and average them before taking a time step.

The second strategy reduces the variance of the gradient estimators such that it is possible to take larger steps with increased values for η and $\alpha\gamma$. On the other hand, a step of the second variant takes longer – if we neglect vector additions, then the computational effort of a single step with the second scheme is the n_b -fold of a single step with the first scheme.

The fair comparison therefore is between $\mathbb{E}[f(x_{n_b n}^{(1)})]$ and $\mathbb{E}[f(x_n^{(2)})]$. Since

$$\sqrt{(4\sigma^2)^2 + 6 \cdot 4\sigma^2 + 9} + 1 = \sqrt{(4\sigma^2 + 3)^2} + 1 = 4(\sigma^2 + 1),$$

we can select $n_0 = 4(\sigma^2 + 1)$ in Theorem 4. Then

$$n_0\gamma\alpha + 2\eta = \frac{n_0\eta}{2(1 + \sigma^2)} + 2\eta = 4\eta = \frac{4}{L(1 + \sigma^2)}, \quad \gamma\alpha = \frac{1}{2L(1 + \sigma^2)^2}.$$

With this choice of n_0 , Theorem 4 yields

$$\begin{aligned} \limsup_{n \rightarrow \infty} \left(n^2 \mathbb{E}[f(x_{n_b n}^{(1)})] \right) &\leq \frac{\frac{4}{L(1 + \sigma^2)} \cdot 4(1 + \sigma^2) \mathbb{E}[(f(x_0) - \inf f) + 2 \mathbb{E}[\|x_0 - x^*\|^2]]}{\frac{1}{2L(1 + \sigma^2)^2} n_b^2} \\ &= \frac{2(1 + \sigma^2)^2}{n_b^2} \{16 \mathbb{E}[f(x_0) - \inf f] + 2L \mathbb{E}[\|x_0 - x^*\|^2]\}. \end{aligned}$$

By the same argument, we find that

$$\limsup_{n \rightarrow \infty} \left(n^2 \mathbb{E}[f(x_{n_b n}^{(2)})] \right) \leq 2 \left(1 + \frac{\sigma^2}{n_b} \right)^2 \{16 \mathbb{E}[f(x_0) - \inf f] + 2L \mathbb{E}[\|x_0 - x^*\|^2]\}$$

with the natural variance scaling. Arguing from the upper bound, the first strategy is therefore clearly superior to the second. Waiting for a better gradient estimate does not pay off.

From the perspective of minimizing the training error, this analysis suggests that the optimal batch size is the largest batch which can be processed fully in parallel. Wu et al. [2018], Masters and Luschi [2018], Wu et al. [2022] find that high stochasticity/small batches are also associated with improved generalization.

With a slight modification, the proof of Theorem 4 extends to the situation of convex objective functions which do not have minimizers.

Theorem 6 (Convexity without minimizers). *Let f be a convex objective function satisfying the assumptions in Section 3.3. Assume that $\eta, \alpha, \gamma, n_0$ and ρ_n are as in Theorem 4. Then $\liminf_{n \rightarrow \infty} \mathbb{E}[f(x_n)] = \inf_{x \in \mathbb{R}^m} f(x)$.*

We conjecture that the statement holds with the limit in place of the lower limit, but that it is impossible to guarantee a rate of convergence $O(n^{-\beta})$ in this setting. The main obstacle are convex functions such as

$$f_\alpha : \mathbb{R} \rightarrow \mathbb{R}, \quad f_\alpha(x) = \begin{cases} x^{-\alpha} & \text{if } x > 1 \\ 1 + \alpha(1 - x) & \text{else} \end{cases},$$

which are very flat and decay very slowly at infinity. Solutions to the heavy ball ODE/continuous time limit of AGNES $x'' = -3/t x' - f'_\alpha(x)$ satisfy $f_\alpha(x(t)) \sim t^{-2\alpha/(2+\alpha)}$, i.e. the decay can be arbitrarily slow if α is close to 0. More details are given in Appendix H.

4. NUMERICAL EXPERIMENTS

4.1. MNIST with LeNet5. We used AGNES as described in Algorithm 3.1 to train a LeNet-5 model due to Lecun et al. [1998] for image classification on the MNIST database of LeCun [1998] in PyTorch. As a loss function we use the cross-entropy loss. The same model was trained with the Adam algorithm of Kingma and Ba [2014] and Stochastic Gradient Descent for comparison.

For all optimizers, the default learning rate of 10^{-3} was used. Adam hyperparameters were set to their default values, and SGD was considered with three versions of momentum $\mu \in \{0, 0.9, 0.99\}$. AGNES was used in two variations: with the default parameters suggested in Algorithm 1 ($\alpha =$

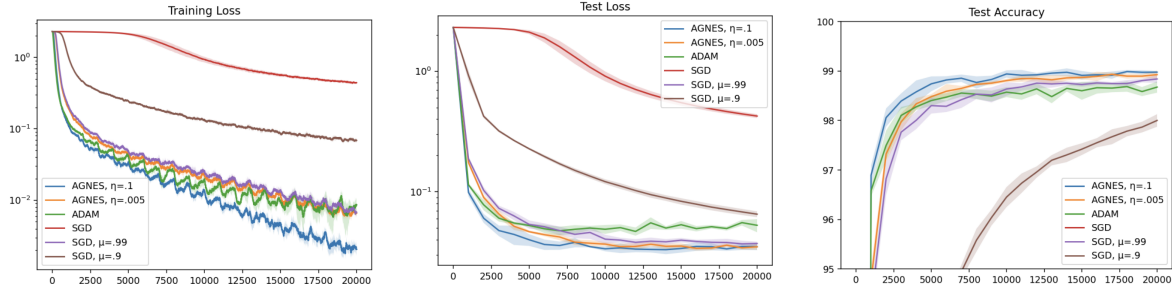


FIGURE 2. AGNES outperforms Adam and SGD (with and without momentum) for the training of LeNet5 on MNIST, both in terms of training loss and test accuracy. SGD without momentum never crosses the 90% accuracy threshold, illustrating that momentum is key to the efficient training of neural networks. The horizontal axis corresponds to the number of time-steps in the optimizer.

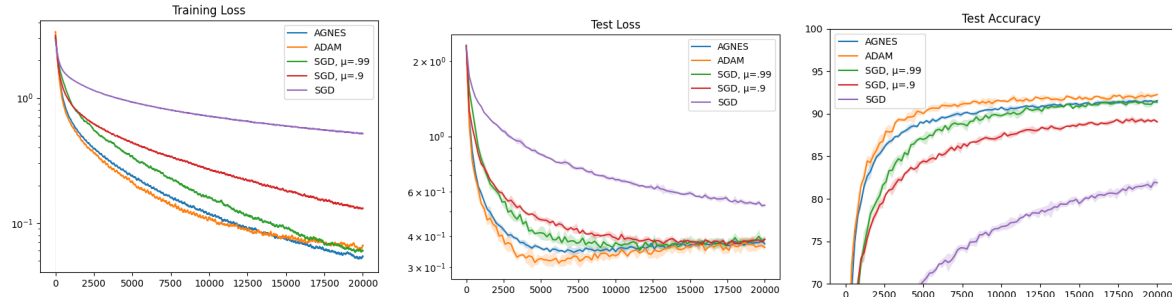


FIGURE 3. AGNES performs comparable to SGD and Adam for the training of ResNet9 on CIFAR-10 with little parameter tuning. Notably, the AGNES test loss and test accuracy lines smoother than the trajectory of other optimizers and achieves lower variation across runs. The horizontal axis corresponds to the number of time-steps in the optimizer.

$10^{-3}, \eta = 5 \times 10^{-3}, \rho = 0.99$), and a more aggressive value $\eta = 0.1$ for the correction step. Stochastic gradients were computed with a batch size of 50. The experiment was repeated 5 times. The average performance is reported in Figure 2. The test loss and accuracy were recorded after every epoch. The training loss and accuracy were estimated by an exponential moving average with decay factor 0.99.

AGNES outperforms Adam and SGD in terms of test accuracy for either of the two values of η , but achieves a higher test accuracy much faster for the aggressive choice $\eta = 0.1$.

4.2. CIFAR-10 with ResNet9. The same experiment was repeated for a larger model on the more complex CIFAR-10 dataset due to Krizhevsky et al. [2009]. We used a 9-layer ResNet (compare He et al. [2016]) based on the implementation of Wright [2019] for this purpose. In line with the original implementation, we used a weight decay value of 10^{-5} for all the optimizers (see Appendix B.4 for a discussion of AGNES with weight decay). Here, the aggressive selection of $\eta = 0.1$ did not perform competitively, and results are not recorded. In this experiment, stochastic gradients were computed with batches of 250 data points. In all other aspects, the experimental set-up is identical to the MNIST experiment.

We find that AGNES converges at a comparable rate as Adam and achieves a similar (but lower) level of accuracy. While SGD with momentum $\mu = 0.99$ seems to catch up eventually, its rate of convergence remains much slower than both AGNES and Adam for most of the training process.

4.3. Convex optimization. A comparison of different optimizers in stochastic convex optimization is given in Appendix A. In the deterministic case AGNES performs comparably to Nesterov’s method or outperforms it, depending on the choice of n_0 . In the stochastic case, AGNES outperforms SGD significantly in accordance with our theoretical guarantees. We do not compare AGNES to Nesterov’s method here, as we do not have theoretical guarantees or insight into how to choose hyperparameters here.

5. CONCLUSION

In this work, we study accelerated gradient descent method with stochastic first order oracles. We consider noise of multiplicative intensity in the gradient oracle and show that this noise model has relevance in overparameterized deep learning applications with ℓ^2 -loss.

Our main contribution is the design and analysis of the AGNES algorithm, a momentum-based gradient descent method which achieves acceleration in convex optimization even with batch size 1 and even if the noise-to-signal ratio in the gradient oracle is extremely large. Choosing suitable constants in Theorem 4, we find that

$$\limsup_{n \rightarrow \infty} (n^2 \mathbb{E}[f(x_n) - \inf f]) \leq 2(1 + \sigma^2)^2 \{ 16 \mathbb{E}[f(x_0) - \inf f] + 2L \mathbb{E}[\|x_0 - x^*\|^2] \},$$

where x^* is a minimizer of f , L is the Lipschitz constant of ∇f and σ measures the stochastic noise intensity in the bound $\mathbb{E}[\|g - \nabla f\|^2] \leq \sigma^2 \|\nabla f\|^2$. By comparison, SGD achieves only

$$\limsup_{n \rightarrow \infty} (n \mathbb{E}[f(x_n) - \inf f]) \leq 2(1 + \sigma^2) \{ \mathbb{E}[f(x_0) - \inf f] + 2L \mathbb{E}[\|x_0 - x^*\|^2] \}$$

under the same assumptions. AGNES can be effectively deployed in deep learning settings. Per time step, it requires one additional vector addition compared to standard implementations of the gradient descent optimizer in PyTorch or TensorFlow with momentum $\mu > 0$, and the same number of operations as the TensorFlow momentum optimizer with Nesterov momentum.

A heuristic consideration would suggest that the momentum step should carry more weight in a high stochasticity setting since random oscillations have a greater chance of cancelling out. Counter-intuitively, the proposed parameter regime in AGNES emphasises the gradient-step more compared to the momentum step as the noise intensity increases, i.e. the larger σ , the smaller $\alpha\gamma/\eta$. We conjecture that this is to a second source of uncertainty: We have a low level of trust in the gradient we observe if σ is large, and additionally we are not confident in asserting where we observed the gradients in previous steps compared to the ‘correct’ deterministic AGNES trajectory. The uncertainty does not only accumulate linearly, but also compositionally through the evaluation of the gradient. In a similar spirit, we observe that AGNES decays faster than SGD asymptotically, but the constants in AGNES grow like σ^4 compared to σ^2 for SGD.

We rigorously prove that the optimal batch size for mini-batches is the largest number of data points which can be processed in parallel, assuming that vector additions take negligible time compared to computing gradient estimates.

To the best of our knowledge, this is the first rigorous study of accelerated gradient descent with noise that degenerates at the set of global minimizers in a general setting.

REFERENCES CITED

Alekh Agarwal, Martin J Wainwright, Peter Bartlett, and Pradeep Ravikumar. Information-theoretic lower bounds on the oracle complexity of convex optimization. *Advances in Neural Information Processing Systems*, 22, 2009.

Guillaume Alain, Nicolas Le Roux, and Pierre-Antoine Manzagol. Negative eigenvalues of the hessian in deep neural networks, 2018. URL <https://openreview.net/forum?id=S1iiddyDG>.

Maksym Andriushchenko, Aditya Vardhan Varre, Loucas Pillaud-Vivien, and Nicolas Flammarion. SGD with large step sizes learns sparse features, 2023. URL <https://openreview.net/forum?id=ipRGZ91NvG4>.

Sanjeev Arora, Simon S Du, Wei Hu, Zhiyuan Li, Russ R Salakhutdinov, and Ruosong Wang. On exact computation with an infinitely wide neural net. In *Advances in Neural Information Processing Systems*, pages 8139–8148, 2019.

Hedy Attouch, Zaki Chbani, Jalal Fadili, and Hassan Riahi. First-order optimization algorithms via inertial systems with hessian driven damping. *Mathematical Programming*, pages 1–43, 2022.

J. F. Aujol, Ch. Dossal, and A. Rondepierre. Convergence rates of the heavy-ball method under the lojasiewicz property. *Mathematical Programming*, 2022a. doi: 10.1007/s10107-022-01770-2. URL <https://doi.org/10.1007/s10107-022-01770-2>.

J.-F. Aujol, Ch. Dossal, and A. Rondepierre. Convergence rates of the heavy ball method for quasi-strongly convex optimization. *SIAM Journal on Optimization*, 32(3):1817–1842, 2022b. doi: 10.1137/21M1403990. URL <https://doi.org/10.1137/21M1403990>.

Raef Bassily, Mikhail Belkin, and Siyuan Ma. On exponential convergence of SGD in non-convex over-parametrized learning. *CoRR*, abs/1811.02564, 2018. URL <http://arxiv.org/abs/1811.02564>.

Amir Beck and Marc Teboulle. A fast iterative shrinkage-thresholding algorithm for linear inverse problems. *SIAM journal on imaging sciences*, 2(1):183–202, 2009.

Mikhail Belkin, Daniel Hsu, Siyuan Ma, and Soumik Mandal. Reconciling modern machine-learning practice and the classical bias–variance trade-off. *Proceedings of the National Academy of Sciences*, 116(32):15849–15854, 2019.

Mikhail Belkin, Daniel Hsu, and Ji Xu. Two models of double descent for weak features. *SIAM Journal on Mathematics of Data Science*, 2(4):1167–1180, 2020.

Albert S Berahas, Jorge Nocedal, and Martin Takáć. A multi-batch l-bfgs method for machine learning. *Advances in Neural Information Processing Systems*, 29, 2016.

Jeremy Bernstein, Yu-Xiang Wang, Kamyar Azizzadenesheli, and Animashree Anandkumar. SIGNSGD: compressed optimisation for non-convex problems. In *Proceedings of the 35th International Conference on Machine Learning, ICML 2018, Stockholmsmässan, Stockholm, Sweden, July 10-15, 2018*, volume 80 of *Proceedings of Machine Learning Research*, pages 559–568. PMLR, 2018. URL <http://proceedings.mlr.press/v80/bernstein18a.html>.

Raghu Bollapragada, Jorge Nocedal, Dheevatsa Mudigere, Hao-Jun Shi, and Ping Tak Peter Tang. A progressive batching l-bfgs method for machine learning. In *International Conference on Machine Learning*, pages 620–629. PMLR, 2018.

Raghu Bollapragada, Tyler Chen, and Rachel Ward. On the fast convergence of minibatch heavy ball momentum. *arXiv preprint arXiv:2206.07553*, 2022.

Leon Bottou, Frank E Curtis, and Jorge Nocedal. Optimization methods for large-scale machine learning. *Siam Review*, 60(2):223–311, 2018.

Sébastien Bubeck, Yin Tat Lee, and Mohit Singh. A geometric alternative to nesterov’s accelerated gradient descent. *CoRR*, abs/1506.08187, 2015. URL <http://arxiv.org/abs/1506.08187>.

Antonin Chambolle and Charles H Dossal. On the convergence of the iterates of FISTA. *Journal of Optimization Theory and Applications*, 166(3):25, 2015.

Daqing Chang, Shiliang Sun, and Changshui Zhang. An accelerated linearly convergent stochastic l-bfgs algorithm. *IEEE transactions on neural networks and learning systems*, 30(11):3338–3346, 2019.

Lénaïc Chizat and Francis Bach. On the global convergence of gradient descent for over-parameterized models using optimal transport. In *Advances in Neural Information Processing Systems*, volume 31. Curran Associates, Inc., 2018. URL <https://proceedings.neurips.cc/paper/2018/file/a1afc58c6ca9540d057299ec3016d726-Paper.pdf>.

PyTorch Contributors. PyTorch Documentation: SGD. <https://pytorch.org/docs/stable/generated/torch.optim.SGD.html>, 2022a. [Online; accessed 8-February-2023].

TensorFlow Contributors. TensorFlow Documentation: SGD. https://www.tensorflow.org/api_docs/python/tf/keras/optimizers/experimental/SGD, 2022b. [Online; accessed 8-February-2023].

Y. Cooper. The loss landscape of overparameterized neural networks, 2019. URL <https://openreview.net/forum?id=SyezvsC5tX>.

Marc Dambrine, Ch Dossal, Bénédicte Puig, and Aude Rondepierre. Stochastic differential equations for modeling first order optimization methods. *HAL preprint hal-03630785*, 2022.

Alex Damian, Tengyu Ma, and Jason D. Lee. Label noise SGD provably prefers flat global minimizers. In *Advances in Neural Information Processing Systems*, 2021. URL <https://openreview.net/forum?id=x2TmPhseWAW>.

Alexandre Défossez, Leon Bottou, Francis Bach, and Nicolas Usunier. A simple convergence proof of adam and adagrad. *Transactions on Machine Learning Research*, 2022. ISSN 2835-8856. URL <https://openreview.net/forum?id=ZPQhzTSWA7>.

Steffen Dereich and Sebastian Kassing. Convergence of stochastic gradient descent schemes for lojasiewicz-landscapes. *arXiv preprint arXiv:2102.09385*, 2021.

Simon S Du, Jason D Lee, Haochuan Li, Liwei Wang, and Xiyu Zhai. Gradient descent finds global minima of deep neural networks. *arXiv:1811.03804 [cs.LG]*, 2018a.

Simon S Du, Xiyu Zhai, Barnabas Poczos, and Aarti Singh. Gradient descent provably optimizes over-parameterized neural networks. *arXiv:1810.02054 [cs.LG]*, 2018b.

Weinan E, Chao Ma, and Lei Wu. A comparative analysis of optimization and generalization properties of two-layer neural network and random feature models under gradient descent dynamics. *Sci. China Math.*, <https://doi.org/10.1007/s11425-019-1628-5>, 2020.

Simon Foucart. *Mathematical Pictures at a Data Science Exhibition*. Cambridge University Press, 2022. doi: 10.1017/9781009003933.

Robert Mansel Gower, Nicolas Loizou, Xun Qian, Alibek Sailanbayev, Egor Shulgin, and Peter Richtárik. Sgd: General analysis and improved rates. In *International conference on machine learning*, pages 5200–5209. PMLR, 2019.

Kaiming He, Xiangyu Zhang, Shaoqing Ren, and Jian Sun. Deep residual learning for image recognition. In *Proceedings of the IEEE conference on computer vision and pattern recognition*, pages 770–778, 2016.

Magnus R Hestenes, Eduard Stiefel, et al. Methods of conjugate gradients for solving linear systems. *Journal of research of the National Bureau of Standards*, 49(6):409–436, 1952.

Arthur Jacot, Franck Gabriel, and Clément Hongler. Neural tangent kernel: Convergence and generalization in neural networks. In *Advances in Neural Information Processing Systems*, volume 31. Curran Associates, Inc., 2018a. URL <https://proceedings.neurips.cc/paper/2018/file/5a4be1fa34e62bb8a6ec6b91d2462f5a-Paper.pdf>.

Arthur Jacot, Franck Gabriel, and Clément Hongler. Neural tangent kernel: Convergence and generalization in neural networks. In *Advances in neural information processing systems*, pages 8571–8580, 2018b.

Prateek Jain, Sham M Kakade, Rahul Kidambi, Praneeth Netrapalli, and Aaron Sidford. Accelerating stochastic gradient descent for least squares regression. In *Conference On Learning Theory*, pages 545–604. PMLR, 2018.

Arnulf Jentzen and Timo Kröger. Convergence rates for gradient descent in the training of overparameterized artificial neural networks with biases. *arXiv preprint arXiv:2102.11840*, 2021.

Richard Jordan, David Kinderlehrer, and Felix Otto. The variational formulation of the fokker–planck equation. *SIAM Journal on Mathematical Analysis*, 29(1):1–17, 1998. doi: 10.1137/S0036141096303359. URL <https://doi.org/10.1137/S0036141096303359>.

Hamed Karimi, Julie Nutini, and Mark Schmidt. Linear convergence of gradient and proximal-gradient methods under the Polyak–Lojasiewicz condition. In *Joint European Conference on Machine Learning and Knowledge Discovery in Databases*, pages 795–811. Springer, 2016.

Rahul Kidambi, Praneeth Netrapalli, Prateek Jain, and Sham Kakade. On the insufficiency of existing momentum schemes for stochastic optimization. In *2018 Information Theory and Applications Workshop (ITA)*, pages 1–9. IEEE, 2018.

Donghwan Kim and Jeffrey A Fessler. Another look at the fast iterative shrinkage/thresholding algorithm (fista). *SIAM Journal on Optimization*, 28(1):223–250, 2018.

Diederik P Kingma and Jimmy Ba. Adam: A method for stochastic optimization. *arXiv preprint arXiv:1412.6980*, 2014.

A. Klenke. *Probability Theory: A Comprehensive Course*. Universitext. Springer London, 2013. ISBN 978-1-4471-5361-0.

Alex Krizhevsky, Geoffrey Hinton, et al. Learning multiple layers of features from tiny images. 2009.

Maxime Laborde and Adam Oberman. A lyapunov analysis for accelerated gradient methods: from deterministic to stochastic case. In *International Conference on Artificial Intelligence and Statistics*, pages 602–612. PMLR, 2020.

Y. Lecun, L. Bottou, Y. Bengio, and P. Haffner. Gradient-based learning applied to document recognition. *Proceedings of the IEEE*, 86(11):2278–2324, 1998. doi: 10.1109/5.726791.

Yann LeCun. The mnist database of handwritten digits. <http://yann. lecun. com/exdb/mnist/>, 1998.

Yann LeCun, Yoshua Bengio, and Geoffrey Hinton. Deep learning. *Nature*, 521(7553):436–444, 2015.

Qianxiao Li, Cheng Tai, and E Weinan. Stochastic modified equations and adaptive stochastic gradient algorithms. In *International Conference on Machine Learning*, pages 2101–2110. PMLR, 2017.

Zhiyuan Li, Tianhao Wang, and Sanjeev Arora. What happens after SGD reaches zero loss? –a mathematical framework. In *International Conference on Learning Representations*, 2022. URL <https://openreview.net/forum?id=siCt4xZn5Ve>.

Kangqiao Liu, Liu Ziyin, and Masahito Ueda. Stochastic gradient descent with large learning rate. *arXiv preprint arXiv:2012.03636*, 2020.

Ilya Loshchilov and Frank Hutter. Fixing weight decay regularization in adam, 2018. URL <https://openreview.net/forum?id=rk6qdGgCZ>.

Ilya Loshchilov and Frank Hutter. Decoupled weight decay regularization. In *International Conference on Learning Representations*, 2019.

Qin Lou, Xuhui Meng, and George Em Karniadakis. Physics-informed neural networks for solving forward and inverse flow problems via the boltzmann-bgk formulation. *Journal of Computational Physics*, 447:110676, 2021.

Dominic Masters and Carlo Luschi. Revisiting small batch training for deep neural networks. *arXiv preprint arXiv:1804.07612*, 2018.

Panayotis Mertikopoulos, Nadav Hallak, Ali Kavis, and Volkan Cevher. On the almost sure convergence of stochastic gradient descent in non-convex problems. *arXiv preprint arXiv:2006.11144*, 2020.

Takashi Mori, Liu Ziyin, Kangqiao Liu, and Masahito Ueda. Logarithmic landscape and power-law escape rate of sgd. *arXiv preprint arXiv:2105.09557*, 2021.

Philipp Moritz, Robert Nishihara, and Michael Jordan. A linearly-convergent stochastic l-bfgs algorithm. In *Artificial Intelligence and Statistics*, pages 249–258. PMLR, 2016.

Yurii Nesterov. A method for solving the convex programming problem with convergence rate $o(1/k^2)$. *Dokl. Akad. Nauk SSSR*, 269:543–547, 1983.

Quynh Nguyen, Mahesh Chandra Mukkamala, and Matthias Hein. On the loss landscape of a class of deep neural networks with no bad local valleys. In *International Conference on Learning Representations*, 2019. URL <https://openreview.net/forum?id=HJgXsjA5tQ>.

Vivak Patel and Albert S Berahas. Gradient descent in the absence of global lipschitz continuity of the gradients: Convergence, divergence and limitations of its continuous approximation. *arXiv preprint arXiv:2210.02418*, 2022.

Vivak Patel and Shushu Zhang. Stochastic gradient descent on nonconvex functions with general noise models. *arXiv preprint arXiv:2104.00423*, 2021.

Scott Pesme, Loucas Pillaud-Vivien, and Nicolas Flammarion. Implicit bias of sgd for diagonal linear networks: a provable benefit of stochasticity. In *Advances in Neural Information Processing Systems*, volume 34, pages 29218–29230. Curran Associates, Inc., 2021. URL <https://proceedings.neurips.cc/paper/2021/file/f4661398cb1a3abd3ffe58600bf11322-Paper.pdf>.

Boris T Polyak. Some methods of speeding up the convergence of iteration methods. *Ussr computational mathematics and mathematical physics*, 4(5):1–17, 1964.

Herbert Robbins and Sutton Monro. A stochastic approximation method. *The annals of mathematical statistics*, pages 400–407, 1951.

Mher Safaryan and Peter Richtárik. Stochastic sign descent methods: New algorithms and better theory. In *International Conference on Machine Learning*, pages 9224–9234. PMLR, 2021.

Itay Safran and Ohad Shamir. Spurious local minima are common in two-layer relu neural networks. In *Proceedings of the 35th International Conference on Machine Learning, ICML 2018, Stockholm, Sweden, July 10-15, 2018*, volume 80 of *Proceedings of Machine Learning Research*, pages 4430–4438. PMLR, 2018. URL <http://proceedings.mlr.press/v80/safran18a.html>.

Levent Sagun, Leon Bottou, and Yann LeCun. Eigenvalues of the hessian in deep learning: Singularity and beyond, 2017. URL <https://openreview.net/forum?id=B186cP9gx>.

Levent Sagun, Utku Evci, V. Ugur Guney, Yann Dauphin, and Leon Bottou. Empirical analysis of the hessian of over-parametrized neural networks, 2018. URL <https://openreview.net/forum?id=rJrTwxbCb>.

Jonathan W Siegel. Accelerated first-order methods: Differential equations and Lyapunov functions. *arXiv preprint arXiv:1903.05671*, 2019.

Umut Simsekli, Ozan Sener, George Deligiannidis, and Murat A Erdogdu. Hausdorff dimension, heavy tails, and generalization in neural networks. In *Advances in Neural Information Processing Systems*, volume 33, pages 5138–5151. Curran Associates, Inc., 2020. URL <https://proceedings.neurips.cc/paper/2020/file/37693cfc748049e45d87b8c7d8b9aacd-Paper.pdf>.

Sebastian U. Stich. Unified Optimal Analysis of the (Stochastic) Gradient Method. *arXiv e-prints*, art. arXiv:1907.04232, July 2019. doi: 10.48550/arXiv.1907.04232.

Sebastian U. Stich and Sai Praneeth Karimireddy. The error-feedback framework: Better rates for sgd with delayed gradients and compressed updates. *J. Mach. Learn. Res.*, 21(1), jun 2022. ISSN 1532-4435.

Weijie Su, Stephen Boyd, and Emmanuel Candes. A differential equation for modeling nesterov’s accelerated gradient method: theory and insights. *Advances in neural information processing systems*, 27, 2014.

Rachel Ward, Xiaoxia Wu, and Leon Bottou. Adagrad stepsizes: Sharp convergence over nonconvex landscapes. In *International Conference on Machine Learning*, pages 6677–6686. PMLR, 2019.

Ashia C Wilson, Ben Recht, and Michael I Jordan. A lyapunov analysis of accelerated methods in optimization. *The Journal of Machine Learning Research*, 22(1):5040–5073, 2021.

Stephan Wojtowytsch. Stochastic gradient descent with noise of machine learning type. Part II: Continuous time analysis. *arXiv:2106.02588 [cs.LG]*, 2021a.

Stephan Wojtowytsch. Stochastic gradient descent with noise of machine learning type. Part I: Discrete time analysis. *arXiv:2105.01650 [stat.ML]*, 2021b.

Matthias Wright. Pytorch resnet9 for cifar-10. <https://github.com/matthias-wright/cifar10-resnet>, 2019. [Online; accessed 8-February-2023].

Lei Wu, Chao Ma, and Weinan E. How sgd selects the global minima in over-parameterized learning: A dynamical stability perspective. *Advances in Neural Information Processing Systems*, 31:8279–8288,

2018.

Lei Wu, Mingze Wang, and Weijie J Su. The alignment property of sgd noise and how it helps select flat minima: A stability analysis. In *Advances in Neural Information Processing Systems*, 2022.

Jingzhao Zhang, Aryan Mokhtari, Suvrit Sra, and Ali Jadbabaie. Direct runge-kutta discretization achieves acceleration. *Advances in neural information processing systems*, 31, 2018.

Pan Zhou, Jiashi Feng, Chao Ma, Caiming Xiong, Steven Hoi, and E. Weinan. Towards theoretically understanding why sgd generalizes better than adam in deep learning. In *Proceedings of the 34th International Conference on Neural Information Processing Systems*, NIPS'20, Red Hook, NY, USA, 2020. Curran Associates Inc. ISBN 9781713829546.

Liu Ziyin, Kangqiao Liu, Takashi Mori, and Masahito Ueda. Strength of minibatch noise in sgd. *arXiv preprint arXiv:2102.05375*, 2021.

Liu Ziyin, Botao Li, James B Simon, and Masahito Ueda. SGD can converge to local maxima. In *International Conference on Learning Representations*, 2022. URL <https://openreview.net/forum?id=9XhPLAjjRB>.

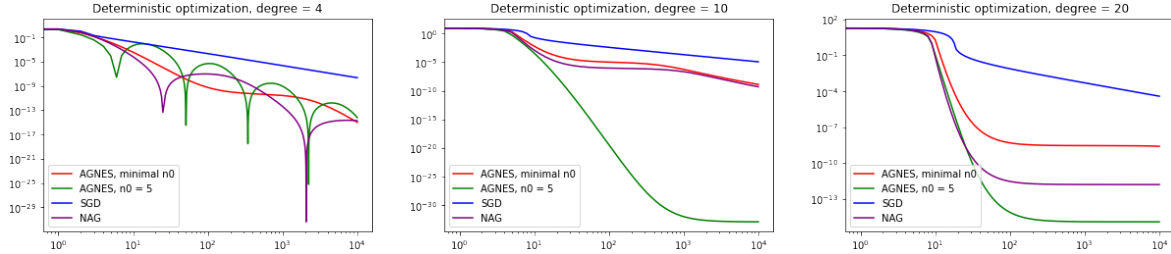


FIGURE 4. All accelerated descent algorithms easily outperform SGD in the deterministic optimization setting for convex objective functions. The minimal parameter $n_0 = \sqrt{10} - 2 \approx 1.16$ does not yield optimal convergence in all cases. A larger choice of n_0 is covered by the theory developed in Theorem 4 and may lead to faster decay in practice. The exact competition between AGNES and NAG may depend in subtle ways on the choice of hyperparameters and the precise objective function.

APPENDIX A. SIMULATIONS CONCERNING CONVEX MINIMIZATION

As an illustration of the AGNES algorithm in the setting most accessible to mathematical analysis, we compare AGNES and SGD (without momentum) in stochastic convex optimization and AGNES, SGD and Nesterov's accelerated gradient descent algorithm

$$x_0 = y_0, \quad x_{n+1} = y_n - \eta \nabla f(y_n), \quad y_{n+1} = x_{n+1} + \frac{n}{n+3}(x_{n+1} - x_n)$$

in deterministic convex optimization. We compare the optimization algorithms for the family of objective functions

$$f_n : \mathbb{R} \rightarrow \mathbb{R}, \quad f_n(x) = \begin{cases} |x|^n & \text{if } |x| < 1, \\ 1 + n(|x| - 1) & \text{else} \end{cases}, \quad n \geq 2$$

and with stochastic gradient estimators $g = (1 + \sigma N) f'(x)$, where N is a unit normal random variable with mean zero and variance 1. Various trajectories are compared for different values of n and σ in Figure 5.

The objective functions are convex (but not strongly convex unless $n = 2$) and have a globally Lipschitz-continuous gradient with constant $L_n = n(n-1)$. The gradient estimators satisfy

$$\mathbb{E}[|g - f'(x)|^2 | x] = \mathbb{E}[|\sigma f'(x)N|^2] = \sigma^2 f'(x)^2 \mathbb{E}[|N|^2] = \sigma^2 f'(x)^2,$$

thus all theoretical results apply. We run AGNES with the parameters derived above and SGD with the optimal step size $\eta = \frac{1}{L(1+\sigma^2)}$ (see Lemma 7 below).

Finally, we present a convergence result for stochastic gradient descent for convex functions with multiplicative noise scaling. To the best of our knowledge, convergence proofs for this type of noise have been given by Bassily et al. [2018], Wojtowytsch [2021b] under a Polyak-Lojasiewicz (or PL) condition (which holds automatically in the strongly convex case), but not for functions which are merely convex. Also this result indicates that optimizers perform comparable to the deterministic case under multiplicative noise.

Analyses of SGD with non-standard noise under various conditions are given by Stich and Karimireddy [2022], Stich [2019].

Lemma 7. *Assume that f is a convex function and that the assumptions laid out in Section 3.3 are satisfied. Consider the sequence x_n be the sequence generated by the gradient descent scheme*

$$x_{n+1} = x_n - \eta g_n, \quad \eta \leq \frac{1}{L(1 + \sigma^2)}.$$

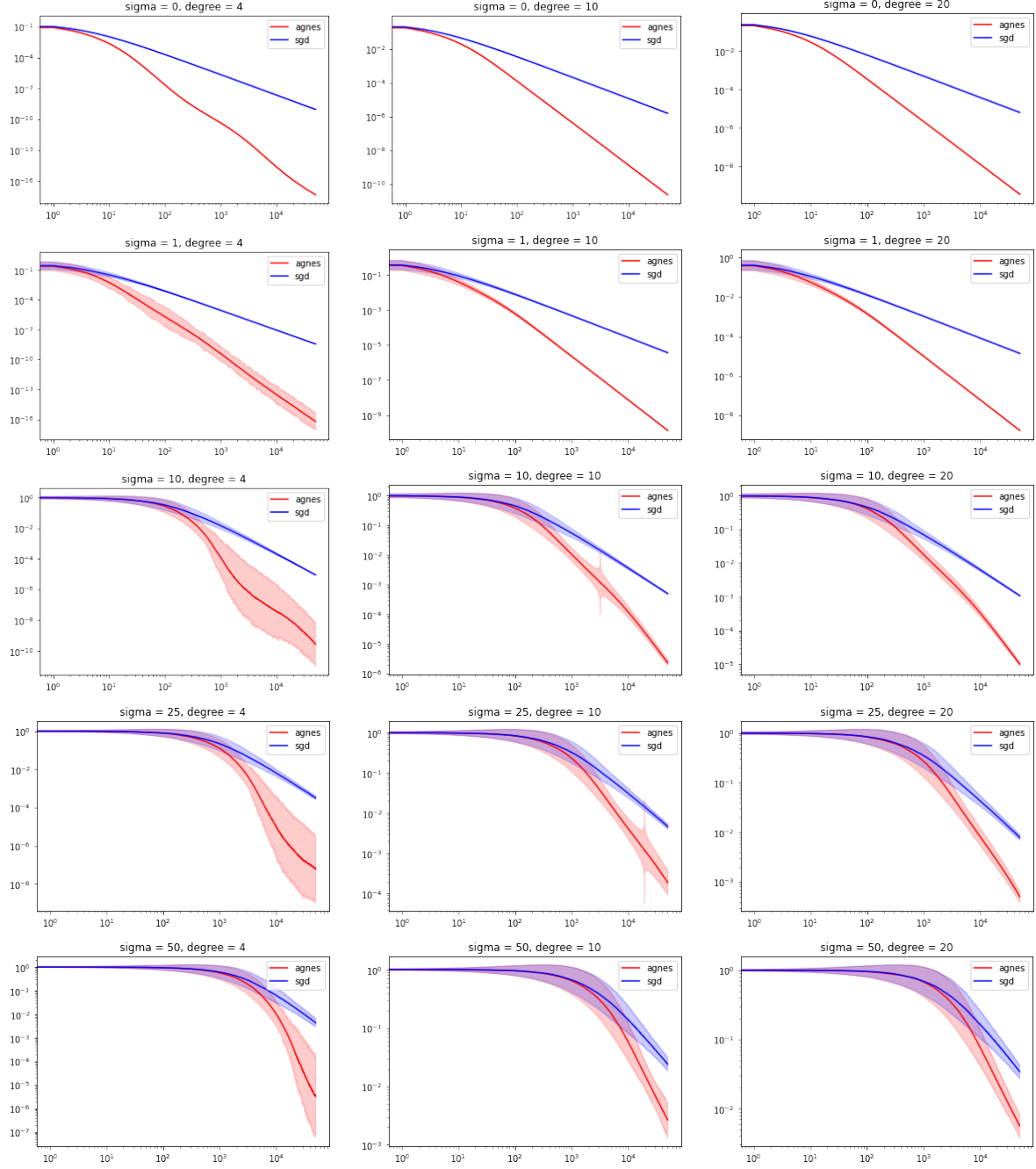


FIGURE 5. We plot $f_n(x_t)$ on a loglog scale for both SGD and AGNES with $n \in \{4, 10, 20\}$ and $\sigma \in \{0, 1, 10, 25, 50\}$. The initial condition is $x_0 = 1$ in all simulations. The error margins are computed as the standard deviation of $\log(f_n(\theta_t))$.

We observe that AGNES (red) significantly outperforms SGD (blue) in all settings. The initial plateau can be viewed in greater detail in Figure 6.

In the late stages of optimization, the confidence interval for $\log(f_n(\theta_t))$ appears to be shrinking as n increases. This is likely due to the fact that the objective functions f_n are ‘flatter’ at the origin as n increases, i.e. a step in the wrong direction is not as detrimental in this setting as for ‘steep’ objectives.

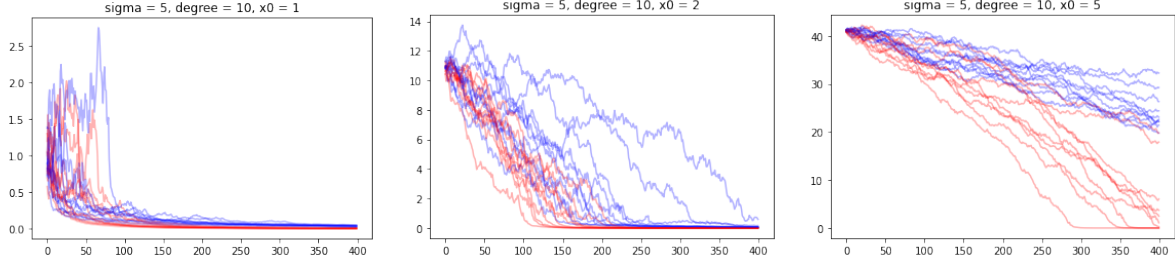


FIGURE 6. We plot $f_n(x_t)$ on a linear scale for both SGD (blue) and AGNES (red) with $n = 10$ and $\sigma = 5$. The initial condition is $x_0 = 1$ in the left plot, $x_0 = 2$ in the middle and $x_0 = 5$ on the right. Here we observe that also on the initial ‘plateau’ observed in Figure 5, AGNES reduces the objective function significantly faster than SGD. However, the logarithm is less sensitive to even large changes at higher magnitudes, and the length of the initial phase is overestimated by the logarithmic time-scale.

On the plateau, the time step size is chosen very pessimistically, since locally f' is Lipschitz constant with any $L > 0$ (since f' is locally constant). The reduction of risk is therefore slow.

Finally, we note that as expected, the trajectories are mostly monotone on large time intervals and remain essentially zero (in the linear scale) once they fall below a certain objective (and noise) threshold.

Then for any $x^* \in \mathbb{R}^m$ the estimate

$$\mathbb{E}[f(x_n) - f(x^*)] \leq \frac{\eta n_0 \mathbb{E}[f(x_0) - f(x^*)] + \frac{1}{2} \mathbb{E}[\|x_0 - x^*\|^2]}{\eta(n + n_0)}.$$

holds for any $n_0 \geq 1 + \sigma^2$. In particular, if $\eta = \frac{1}{L(1+\sigma^2)}$ and $n_0 = 1 + \sigma^2$, then

$$\mathbb{E}[f(x_n) - f(x^*)] \leq (1 + \sigma^2) \frac{\mathbb{E}[f(x_0) - f(x^*)] + \frac{L}{2} \mathbb{E}[\|x_0 - x^*\|^2]}{n + 1 + \sigma^2}.$$

This is particularly meaningful if there exists x^* such that $f(x^*) = \inf f$, in which case the first term is non-negative.

Proof. In the proof, we anticipate identities for conditional expectations, which are reviewed in Appendix F. Let $n_0 \geq 0$ and consider the Lyapunov sequence

$$\mathcal{L}_n = \mathbb{E} \left[\eta(n + n_0)(f(x_n) - \inf f) + \frac{1}{2} \|x_n - x^*\|^2 \right]$$

We find that

$$\begin{aligned} \mathcal{L}_{n+1} &= \mathbb{E} \left[\eta(n + n_0 + 1) \{f(x_n - \eta g_n) - \inf f\} + \frac{1}{2} \|x_n - \eta g_n - x^*\|^2 \right] \\ &\leq \mathbb{E} \left[\eta(n + n_0 + 1) \left\{ f(x_n) - \frac{\eta}{2} \|\nabla f(x_n)\|^2 - \inf f \right\} + \frac{1}{2} \|x_n - x^*\|^2 - \eta(x_n - x^*) \cdot g_n + \frac{\eta^2}{2} \|g_n\|^2 \right] \\ &= \mathbb{E} \left[\eta(n + n_0) \{f(x_n) - \inf f\} + \frac{1}{2} \|x_n - x^*\|^2 + f(x_n) - \inf f + \eta \nabla f(x_n) \cdot (x^* - x_n) \right. \\ &\quad \left. - \frac{\eta^2(n + n_0)}{2} \|\nabla f(x_n)\|^2 + \frac{\eta^2}{2} \|g_n\|^2 \right] \\ &\leq \mathcal{L}_n + 0 - \frac{\eta^2}{2} (n + n_0 - (1 + \sigma^2)) \mathbb{E}[\|\nabla f(x_n)\|^2] \end{aligned}$$

by the convexity of f . The result therefore holds if n_0 is chosen large since

$$\mathbb{E}[f(x_n) - f(x^*)] \leq \frac{\mathcal{L}_n}{\eta(n + n_0)} \leq \frac{\mathcal{L}_0}{\eta(n + n_0)} = \frac{\eta n_0 \mathbb{E}[f(x_0) - f(x^*)] + \frac{1}{2} \mathbb{E}[\|x_0 - x^*\|^2]}{\eta(n + n_0)}.$$

□

APPENDIX B. AGNES AND THE SGD OPTIMIZER IN PYTORCH AND TENSORFLOW

In this appendix, we compare the AGNES momentum scheme to optimizers which are currently implemented in the TensorFlow (v2.11.0) and PyTorch (v1.13.1) libraries as documented by Contributors [2022b] and Contributors [2022a] respectively.

B.1. Nesterov = False. The Tensorflow momentum optimizer with standard (non-Nesterov) momentum proceeds along the time-stepping scheme

$$(B.1) \quad v_{n+1} = \mu v_n - \eta g_n, \quad x_{n+1} = x_n + v_{n+1},$$

where g_n is an estimate of $\nabla f(x_n)$. The PyTorch momentum optimizer scheme is

$$(B.2) \quad v_{n+1} = \mu v_n + (1 - \tau)g_n, \quad x_{n+1} = x_n - \gamma v_n.$$

Also here, g_n is an estimator for $\nabla f(x_n)$. The schemes are differently parametrized versions of the same time-stepping scheme.

Lemma 8. *Assume that (x_n^{TF}, v_n^{TF}) and (x_n^{PT}, v_n^{PT}) follow the iteration scheme (B.1) and (B.2) respectively. If $v_0^{TF} = v_0^{PT} = 0$ and $x_0^{TF} = x_0^{PT}$ and the parameters satisfy*

$$(B.3) \quad (1 - \tau^{PT})\gamma^{PT} = \eta^{TF}, \quad \mu^{PT} = \mu^{TF}$$

then

$$(B.4) \quad \eta^{-1} v_n^{TF} = -(1 - \tau)^{-1} v_n^{PT}, \quad x_n^{TF} = x_n^{PT} \quad \forall n \in \mathbb{N}.$$

The equality holds exactly if g_n is deterministic (or the randomness is accounted for correctly), otherwise it holds in distribution. We currently assume that if $x_n^{TF} = x_n^{PT}$, then $g_n^{TF} = g_n^{PT}$.

Proof. The equations hold at initialization $n = 0$ by assumption. We proceed by induction. If (B.3) holds and (B.4) holds for $n \in \mathbb{N}$, then

$$\begin{aligned} \eta^{-1} v_{n+1}^{TF} &= \mu \eta^{-1} v_n^{TF} - g_n \\ &= -\mu(1 - \tau)^{-1} v_n^{PT} - g_n \\ &= -(1 - \tau)^{-1} (\mu v_n^{PT} + (1 - \tau)g_n) \\ &= -(1 - \tau)^{-1} v_{n+1}^{PT} \\ x_{n+1}^{TF} &= x_n^{TF} + v_{n+1}^{TF} \\ &= x_n^{PT} - \frac{\eta}{1 - \tau} v_{n+1}^{PT} \\ &= x_n^{PT} - \gamma v_{n+1}^{PT} \\ &= x_{n+1}^P. \end{aligned}$$

□

It therefore suffices to compare AGNES to the Tensorflow SGD optimizer. Essentially, we demonstrate that SGD with non-Nesterov momentum can be considered a special case of AGNES.

Lemma 9. Assume that (x_n^{TF}, v_n^{TF}) and $(x_n^{AG}, x'_n, v_n^{AG})$ follow the iteration scheme (B.1) and the AGNES scheme

$$x'_n = x_n^{AG} + \alpha v_n^{AG}, \quad v_{n+1}^{AG} = \rho(v_n^{AG} - \gamma g_n), \quad x_{n+1}^{AG} = x'_n - \eta g_n.$$

respectively. If $v_0^{TF} = v_0^{PT} = 0$ and $x_0^{TF} = x_0^{AG}$ and the parameters satisfy

$$(B.5) \quad \eta^{AG} = 0, \quad \mu = \rho, \quad \eta^{TF} = \rho\gamma, \quad \alpha = 1$$

then

$$(B.6) \quad x_{n+1}^{AG} = x'_n, \quad x_{n+1}^{AG} = x_n^{TF}, \quad v_n^{TF} = v_n^{AG} \quad \forall n \in \mathbb{N}_0.$$

Proof. The identity $x_{n+1}^{AG} = x'_n$ holds trivially since $\eta^{AG} = 0$. In particular, g_n is an oracle for $\nabla f(x'_n) = \nabla f(x_{n-1})$. For the identities, we proceed by induction.

Note that $x_1^{AG} = x'_0 = x_0$ since $v_0^{AG} = 0$. For $n \geq 1$, we compute that

$$x_{n+1}^{AG} = x_n^{AG} + \alpha v_n^{AG} = x_{n-1}^{TF} + v_n^{TF} = x_n^{TF}$$

by the induction hypothesis and the fact that $\alpha = 1$. Furthermore

$$v_{n+1}^{AG} = \rho(v_n^{AG} - \gamma g_n) = \mu v_n^{TF} - \mu\gamma g_n = \mu v_n^{TF} - \eta^{TF} g_n = v_{n+1}^{TF}.$$

This concludes the proof. \square

Thus AGNES generalizes the vanilla momentum version of SGD as it is currently implemented by the major machine learning libraries.

B.2. Nesterov = True. The Tensorflow momentum optimizer with Nesterov momentum proceeds along the time-stepping scheme

$$(B.7) \quad v_{n+1} = \mu v_n - \eta g_n, \quad x_{n+1} = x_n + \mu v_{n+1} - \eta g_n$$

where g_n is an estimate of $\nabla f(x_n)$. The PyTorch variation of a Nesterov momentum optimizer is given by the scheme

$$(B.8) \quad \tilde{v}_{n+1} = \mu v_n + (1 - \tau) g_n, \quad v_{n+1} = g_n + \mu \tilde{v}_{n+1} = \mu^2 v_n + (1 + \mu(1 - \tau)) g_n, \quad x_{n+1} = x_n - \gamma v_n.$$

Also here, g_n is an estimator for $\nabla f(x_n)$. These schemes are *not* equivalent. In fact, the Nesterov momentum optimizer of PyTorch is equivalent to the regular momentum optimizer laid out in (B.2) under obvious parameter substitutions. Again, it therefore suffices to compare AGNES to the Nesterov version of the TensorFlow optimizer.

Lemma 10. Assume that (x_n^{TF}, v_n^{TF}) and $(x_n^{AG}, x'_n, v_n^{AG})$ follow the iteration scheme (B.7) and the AGNES scheme

$$x'_n = x_n^{AG} + \alpha v_n^{AG}, \quad v_{n+1} = \rho(v_n^{AG} - \gamma g_n), \quad x_{n+1}^{AG} = x'_n - \eta g_n.$$

respectively. If $v_0^{TF} = v_0^{PT} = 0$ and $x_0^{TF} = x_0^{AG}$ and the parameters satisfy

$$(B.9) \quad \eta^{AG} = \eta^{TF}, \quad \mu = \rho, \quad \eta = \gamma\alpha$$

then

$$(B.10) \quad x'_n = x_n^{TF}, \quad \mu v_n^{TF} = \alpha v_n^{AG} \quad \forall n \in \mathbb{N}_0.$$

Proof. Again, we proceed by induction. Note that $x'_0 = x_0^{AG} = x_0^{TF}$ since $v_0^{AG} = 0$. We now find that

$$\begin{aligned}\alpha v_{n+1}^{AG} &= \alpha \rho(v_n^{AG} - \gamma g_n) \\ &= \mu(\alpha v_n^{AG} - \alpha \gamma g_n) \\ &= \mu(\mu v_n^{TF} - \eta g_n) \\ &= \mu v_{n+1}^{TF} \\ x'_{n+1} &= x_{n+1}^{AG} + \alpha v_{n+1}^{AG} \\ &= x'_n - \eta g_n + \alpha v_{n+1}^{AG} \\ &= x_n^{TF} - \eta g_n + \mu v_{n+1}^{TF} \\ &= x_{n+1}^{TF}.\end{aligned}$$

□

In particular, SGD with Nesterov momentum as implemented in TensorFlow can be considered as a special case of AGNES with $\alpha\gamma = \eta$. Additionally, in this implementation we only access the sequence of auxiliary points x'_n rather than the sequence of points x_n for which we derive rigorous guarantees. As discussed previously, this is also the case in our implementation of AGNES, as it facilitates the regular PyTorch workflow of computing gradients outside the optimizer.

It is, however, a simple endeavour to compute $x_{n+1} = x'_n - \eta g_n$ from x'_n by adding a gradient step after the last iteration. Thus all major implementations of the SGD optimizer can be considered a special case of AGNES in the case $\eta = 0$ or $\eta = \alpha\gamma$. As our proofs suggest, the regime $\alpha\gamma < \eta$ is better suited to achieving accelerated rates.

B.3. Multiple optimizers. According to Lemma 10, we can decompose one AGNES step with parameters $\eta, \alpha, \gamma, \rho$ into two steps with different optimizers in Tensorflow, which share the same state dictionary and use the same gradient estimate:

- (1) One step with SGD with parameters
 - learning rate = $\alpha\gamma$
 - momentum = ρ
 - nesterov = True
- (2) One step with SGD with parameters
 - learning rate = $\eta - \alpha\gamma > 0$.
 - momentum = 0.

Both optimizers share the same gradient estimate g_n computed at the current parameters. For the final point, we return the update *after* the step with the pure gradient descent optimizer.

B.4. Weight decay. Weight decay is a machine learning tool which controls the magnitude of the coefficients of a neural network. In the simplest SGD setting, weight decay takes the form of a modified update step

$$x_{n+1} = (1 - \lambda\eta)x_n - \eta g_n$$

for $\lambda > 0$. This corresponds to computing with a modified objective function $x \mapsto f(x) + \frac{\lambda}{2} \|x\|^2$ and using gradient estimates which are stochastic for f and deterministic for the second term. In GD, both perspectives coincide unconditionally.

In advanced minimizers, the two perspectives no longer coincide. For Adam, Loshchilov and Hutter [2018, 2019] initiated a debate on the superior strategy of including weight decay. We note that the two strategies do not coincide for AGNES, but do not comment on the superiority of one over the other:

- (1) Treating weight decay as a dynamic property of the optimizer leads to an update rule like

$$x'_n = x_n + \alpha v_n, \quad v_{n+1} = \rho(v_n - \gamma g_n), \quad x_{n+1} = (1 - \lambda\eta)x_n - \eta g_n.$$

(2) Treating weight decay as a component of the objective function to be minimized leads to the update rule

$$x'_n = x_n + \alpha v_n, \quad v_{n+1} = \rho(v_n - \gamma g_n - \gamma \lambda x'_n), \quad x_{n+1} = (1 - \lambda \eta)x'_n - \eta g_n.$$

In many situations the same continuous dynamics can be interpreted in various ways. For example, Jordan et al. [1998] show that the heat equation is both the L^2 -gradient flow of the Dirichlet energy and the Wasserstein gradient flow of the entropy function. Whether or not a term in the gradient flow equation is considered part of the dissipation or the energy to be minimized may be a question of the underlying mathematical model and physical phenomenon more than a question of interpreting a differential equation. Similarly, we maintain that either discretization has validity in this setting, albeit with different interpretations. In our numerical experiments, we choose the second approach, viewing weight decay as a property of the objective function rather than the dissipation. This coincides with the approach taken by the SGD (and SGD with momentum) optimizer as well as Adam (but not AdamW).

APPENDIX C. PROOF OF LEMMA 1: SCALING INTENSITY OF MINIBATCH NOISE

In this appendix, we provide theoretical justification for the multiplicative noise scaling regime considered in this article. Recall our main statement:

Lemma 11 (Noise intensity). *Assume that $\ell(h, y) = \|h - y\|^2$ and $f : \mathbb{R}^m \rightarrow \mathbb{R}^k$ satisfies*

$$\|\nabla_w h(w, x_i)\|^2 \leq C(1 + \|w\|)^p \quad \forall w \in \mathbb{R}^m, i = 1, \dots, n$$

for some $C, p > 0$. Then

$$\frac{1}{n} \sum_{i=1}^n \|\nabla \ell_i - \nabla \mathcal{R}\|^2 \leq C^2 (1 + \|w\|)^{2p} \mathcal{R}(w) \quad \forall w \in \mathbb{R}^m.$$

Proof. Since $\nabla \mathcal{R} = \frac{1}{n} \sum_{i=1}^n \nabla \ell_i$, we observe that

$$\frac{1}{n} \sum_{i=1}^n \|\nabla \ell_i - \nabla \mathcal{R}\|^2 \leq \frac{1}{n} \sum_{i=1}^n \|\nabla \ell_i\|^2$$

as the average of a quantity is the unique value which minimizes the mean square discrepancy: $\mathbb{E}X = \operatorname{argmin}_{a \in \mathbb{R}} \mathbb{E}[|X - a|^2]$. We further find by Hölder's inequality that

$$\begin{aligned} \frac{1}{n} \sum_{i=1}^n \|\nabla \ell_i\|^2 &= \frac{1}{n} \sum_{i=1}^n \left\| \sum_{j=1}^k (h_k(w, x_i) - y_{i,k}) \nabla_w h_k(w, x_i) \right\|^2 \\ &\leq \frac{1}{n} \sum_{i=1}^n \left(\sum_{k=1}^n h_k(w, x_i) - y_{i,k} \right)^2 \left(\sum_{k=1}^n \|\nabla_w h(w, x_i)\|^2 \right) \\ &\leq C^2 (1 + \|w\|^2)^{2p} \frac{1}{n} \sum_{i=1}^n \|h(w, x_i) - y_i\|_2^2 \\ &= C^2 (1 + \|w\|^2)^{2p} \mathcal{R}(w). \end{aligned}$$

□

APPENDIX D. NON-CONVEXITY IN DEEP LEARNING

In this section we prove two statements which illustrate that in general, optimization landscapes in deep learning *cannot* be convex.

Lemma 12 (Loss landscape). (1) Assume that $\mathcal{R} : \mathbb{R}^m \rightarrow [0, \infty)$ is a loss function and \mathcal{M} is an n -dimensional manifold such that $\mathcal{R}(w) = 0$ if and only if $w \in \mathcal{M}$.

If $w \in \mathcal{M}$ and $\mathcal{R} : B_r(w) \rightarrow \mathbb{R}$ is convex, then $\mathcal{M} \cap B_r(w) = (w + T_w \mathcal{M}) \cap B_r(w)$, i.e. \mathcal{M} is perfectly straight at w .

(2) If the parameterized function h is C^2 -smooth in the weight variables w and the risk function $\mathcal{R}(w) = \frac{1}{n} \sum_{i=1}^n (h(w, x_i) - y_i)^2$ is convex for all $y \in \mathbb{R}^n$, then the map $w \mapsto h(w, x_i)$ is linear for all $i = 1, \dots, n$.

Lemma 12 is a partial refinement of [Wojtowytsch, 2021b, Corollary A.1]. Strictly negative eigenvalues of $D^2 \mathcal{R}$ have been observed numerically close to the set of minimizers by Sagun et al. [2017, 2018], Alain et al. [2018], but tend to 0 as one approaches the set of minimizers.

Proof. **First claim.** Without loss of generality, assume that $w = 0$. If $w' \in B_r(0) \cap \mathcal{M}$, then $w(t) := tw' = tw' + (1-t)0$ satisfies

$$0 \leq \mathcal{R}(w(t)) \leq t\mathcal{R}(w') + (1-t)\mathcal{R}(0) = 0 \quad \forall t \in [0, 1]$$

since $w(t) \in B_r(0)$ for all $t \in [0, 1]$ and $\mathcal{R} : B_r(w) \rightarrow \mathbb{R}$ is convex. In particular $w' = w'(0) \in T_0 \mathcal{M}$ by definition, i.e. $\mathcal{M} \cap B_r(0) \subseteq (T_0 \mathcal{M}) \cap B_r(0)$ by the definition of the tangent space. On the other hand, since \mathcal{M} is an n -dimensional manifold contained in the linear space $T_0 \mathcal{M}$ and \mathcal{M} has no boundary, we find that the two sets coincide.

Second claim. Assume that h is not linear in the variables w , i.e. there exists $I \in \{1, \dots, n\}$ and $\bar{w} \in \mathbb{R}^m$ such that $D^2 h(\bar{w}, x_I) \neq 0$. We compute the Hessian of the risk function \mathcal{R}_y with given labels y :

$$D^2 \mathcal{R}_y(\bar{w}) = \frac{2}{n} \sum_{i=1}^n (h(\bar{w}, x_i) - y_i) D_w^2 h(\bar{w}, x_i) + \frac{2}{n} \sum_{i=1}^n \nabla_w h(\bar{w}, x_i) \otimes \nabla_w h(\bar{w}, x_i).$$

The second term is always non-negative semi-definite, while the first term may or may not be non-negative. Consider any labels y_i for $i \neq I$. We observe that

$$\lim_{y_I \rightarrow \pm\infty} \frac{1}{y_I} D^2 \mathcal{R}_y(\bar{w}) = -D^2 h(\bar{w}, x_I).$$

In particular, if y_I is either large positive or large negative, then $D^2 \mathcal{R}_y(\bar{w}) = -y_I D^2 h(\bar{w}, x_I) + O(1)$ fails to be non-negative semi-definite. \square

APPENDIX E. PROOF OF LEMMA 2: ELEMENTARY OBSERVATIONS ON THE DESCENT ALGORITHM

Here we prove that α, γ can be reduced to a single parameter since only $\alpha\gamma$ matters to the descent algorithm. Recall the precise statement:

Lemma 13. Let $\rho \in (0, 1)$ and $\eta > 0$ parameters. Assume that α, γ and $\tilde{\alpha}, \tilde{\gamma}$ are parameters such that $\tilde{\alpha}\tilde{\gamma} = \alpha\gamma$. Consider the sequences $(\tilde{x}_n, \tilde{x}'_n, \tilde{v}_n)$ and (x_n, x'_n, v_n) generated by the time stepping scheme with parameters $(\rho, \eta, \tilde{\alpha}, \tilde{\gamma})$ and $(\rho, \eta, \alpha, \gamma)$ respectively. If $x_0 = \tilde{x}_0$ and $\alpha v_0 = \tilde{\alpha} \tilde{v}_0$, then $x_n = \tilde{x}_n$, $x'_n = \tilde{x}'_n$ and $\tilde{\alpha} \tilde{v}_n = \alpha v_n$ for all $n \in \mathbb{N}$.

Proof. We proceed by mathematical induction on n . For $n = 0$, the claim holds by the hypotheses of the lemma. For the inductive hypothesis, we suppose that $x_n = \tilde{x}_n$ and $\alpha v_n = \tilde{\alpha} \tilde{v}_n$ and prove the claim for $n + 1$. Note that since $x'_n = x_n + \alpha v_n$, it automatically follows that $x'_n = \tilde{x}'_n$. This implies that

$$x_{n+1} = x'_n - \eta g_n = \tilde{x}'_n - \eta g_n = \tilde{x}_{n+1}.$$

Considering the velocity term,

$$\alpha v_{n+1} = \rho_n (\alpha v_n - \alpha\gamma g_n) = \rho_n (\tilde{\alpha} \tilde{v}_n - \tilde{\alpha} \tilde{\gamma} g_n) = \tilde{\alpha} \rho_n (\tilde{v}_n - \tilde{\gamma} g_n) = \tilde{\alpha} \tilde{v}_{n+1}$$

Thus $x_{n+1} = \tilde{x}_{n+1}$ and $\alpha v_{n+1} = \tilde{\alpha} \tilde{v}_{n+1}$. The induction can therefore be continued. \square

APPENDIX F. BACKGROUND MATERIAL AND AUXILIARY RESULTS

In this appendix, we gather a few auxiliary results that will be used in the proofs below. We believe that these will be familiar to the experts and can be skipped by experienced readers.

Let us record a modified gradient descent estimate used below. The difference to the usual estimate is that the gradient is evaluated at the terminal point of the interval rather than the initial point.

Lemma 14. *For any x, v and α : If f is L -smooth, then*

$$f(x + \alpha v) \leq f(x) + \alpha \nabla f(x + \alpha v) \cdot v + \frac{L\alpha^2}{2} \|v\|^2.$$

Proof. The proof is essentially identical to that standard decay estimate. We compute

$$\begin{aligned} f(x) &= f(x + \alpha v) - \int_0^\alpha \frac{d}{dt} f(x + tv) dt \\ &= f(x + \alpha v) - \int_0^\alpha [\nabla f(x + \alpha v) + \{\nabla f(x + tv) - \nabla f(x + \alpha v)\}] \cdot v dt \\ &\geq f(x + \alpha v) - \nabla f(x + \alpha v) \cdot v - \int_0^\alpha L(\alpha - t) \|v\|^2 \\ &= f(x + \alpha v) - \alpha \nabla f(x + \alpha v) \cdot v - \frac{L\alpha^2}{2} \|v\|^2. \end{aligned}$$

□

Finally, we turn towards a very brief review of the stochastic process theory used in the analysis of gradient descent type algorithms.

Recall that conditional expectations are a technical tool to capture the stochasticity in a random variable X which can be predicted from another random quantity Y . This allows us to quantify the randomness in the gradient estimators g_n which comes from the fact that x_n is a random variable (not known ahead of time) and which randomness comes from the fact that on top of the inherent randomness due to e.g. initialization, we do not compute exact gradients. In particular, even at run time when x_n is known, there is additional noise in the estimators g_n in our setting.

We denote by \mathcal{F}_n all information that is known after taking n gradient steps, i.e. $\mathbb{E}[g_n | \mathcal{F}_n]$ is the mean of g_n if all previous steps are already known. For a more thorough introduction to filtrations and conditional expectations, see e.g. [Klenke, 2013, Chapter 8].

In the next Lemma, we recall two important properties of conditional expectations.

Lemma 15. [Klenke, 2013, Theorem 8.14] *Let g and h be random variables and \mathcal{F} be a σ -algebra. Then the conditional expectations $\mathbb{E}[g | \mathcal{F}]$ and $\mathbb{E}[h | \mathcal{F}]$ satisfy the following properties:*

- (1) (linearity) $\mathbb{E}[\alpha g + \beta h | \mathcal{F}] = \alpha \mathbb{E}[g | \mathcal{F}] + \beta \mathbb{E}[h | \mathcal{F}]$ for all $\alpha, \beta \in \mathbb{R}$
- (2) (tower identity) $\mathbb{E}[\mathbb{E}[g | \mathcal{F}]] = \mathbb{E}[g]$
- (3) If g is \mathcal{F} -measurable then $\mathbb{E}[gh | \mathcal{F}] = g \mathbb{E}[h | \mathcal{F}]$. In particular, $\mathbb{E}[g | \mathcal{F}] = g$

We note two small applications of these properties.

Lemma 16. *Suppose g_n, x_n , and x'_n satisfy the assumptions laid out in Section 3.3, then the following statements hold*

- (1) $\mathbb{E}[\|g_n\|^2] = (1 + \sigma^2) \mathbb{E}[\|\nabla f(x'_n)\|^2]$
- (2) $\mathbb{E}[\nabla f(x'_n) \cdot g_n] = \mathbb{E}[\|\nabla f(x'_n)\|^2]$

Proof. Let \mathcal{F}_n be the σ -algebra generated by (x_n, x'_n, v_n) as in Section 3.3. The first result then follows by an application of the tower identity with \mathcal{F}_n , expanding the square of the norm as a dot product,

and then using the linearity of conditional expectation.

$$\begin{aligned}
\mathbb{E} [\|g_n\|^2] &= \mathbb{E} [\mathbb{E} [\|g_n\|^2 \mid \mathcal{F}_n]] \\
&= \mathbb{E} [\mathbb{E} [\|g_n - \nabla f(x'_n)\|^2 + 2g \cdot \nabla f(x'_n) - \|\nabla f(x'_n)\|^2 \mid \mathcal{F}_n]] \\
&= \mathbb{E} [\mathbb{E} [\|g_n - \nabla f(x'_n)\|^2 \mid \mathcal{F}_n]] + 2\mathbb{E} [g \cdot \nabla f(x'_n) \mid \mathcal{F}_n] - \mathbb{E} [\|\nabla f(x'_n)\|^2 \mid \mathcal{F}_n] \\
&\leq \mathbb{E} [\sigma^2 \nabla f(x'_n) + 2\|\nabla f(x'_n)\|^2 - \|\nabla f(x'_n)\|^2] \\
&= (1 + \sigma^2) \mathbb{E} [\|\nabla f(x'_n)\|^2].
\end{aligned}$$

For the second result, we observe that since f is a deterministic function and x'_n is \mathcal{F}_n -measurable, $\nabla f(x'_n)$ is also measurable with respect to the σ -algebra. Then using the tower identity followed by the third property in Lemma 15,

$$\begin{aligned}
\mathbb{E} [\nabla f(x'_n) \cdot g_n] &= \mathbb{E} [\mathbb{E} [\nabla f(x'_n) \cdot g_n \mid \mathcal{F}_n]] \\
&= \mathbb{E} [\nabla f(x'_n) \cdot \mathbb{E} [g_n \mid \mathcal{F}_n]] \\
&= \mathbb{E} [\nabla f(x'_n) \cdot \nabla f(x'_n)] \\
&= \mathbb{E} [\|\nabla f(x'_n)\|^2].
\end{aligned}$$

□

As a consequence, we note the following decrease estimate.

Lemma 17. *Suppose that f, x'_n, x_n , and g_n satisfy the conditions laid out in Section 3.3, then*

$$\mathbb{E} [f(x'_n - \eta g_n)] \leq \mathbb{E} [f(x'_n)] - \eta \left(1 - \frac{L(1 + \sigma^2)\eta}{2}\right) \mathbb{E} [\|\nabla f(x'_n)\|^2].$$

Proof. Using L -smoothness of f ,

$$f(x'_n - \eta g_n) \leq f(x'_n) - \eta g_n \cdot \nabla f(x'_n) + \frac{L\eta^2}{2} \|g\|^2.$$

Then taking the expectation and using the results of the previous lemma,

$$\begin{aligned}
\mathbb{E} [f(x'_n - \eta g_n)] &\leq \mathbb{E} [f(x'_n)] - \eta \mathbb{E} [\|\nabla f(x'_n)\|^2] + \frac{L\eta^2}{2} (1 + \sigma^2) \mathbb{E} [\|\nabla f(x'_n)\|^2] \\
&\leq \mathbb{E} [f(x'_n)] - \eta \left(1 - \frac{L(1 + \sigma^2)\eta}{2}\right) \mathbb{E} [\|\nabla f(x'_n)\|^2]
\end{aligned}$$

□

In particular, if $\eta \leq \frac{1}{L(1 + \sigma^2)}$, then

$$\mathbb{E} [f(x - \eta g)] \leq \mathbb{E} [f(x)] - \frac{\eta}{2} \mathbb{E} [\|\nabla f(x)\|^2].$$

APPENDIX G. PROOF OF THEOREM 3: NON-CONVEX OPTIMIZATION

Let us recall the formulation of Theorem 3.

Theorem 3 (Non-convex case). *Assume that f satisfies the assumptions laid out in Section 3.3. Let $\eta, \alpha, \gamma, \rho$ be such that*

$$\eta \leq \frac{1}{L(1 + \sigma^2)}, \quad \alpha\gamma < \frac{\eta}{1 + \sigma^2}, \quad (L\alpha\gamma + 1)\rho^2 \leq 1.$$

Then

$$\min_{1 \leq i \leq n} \mathbb{E} [\|\nabla f(x_i)\|^2] \leq \frac{2\mathbb{E} [f(x_1) - \inf f + \frac{1}{\alpha\gamma\rho^2} \|v_1\|^2]}{n (\eta - \alpha\gamma(1 + \sigma^2))}.$$

In particular, consider the setting

$$\eta = \frac{1}{L(1+\sigma^2)}, \quad \alpha\gamma = \frac{\eta}{2(1+\sigma^2)} = \frac{1}{2L(1+\sigma^2)^2}$$

Then

$$(L\alpha\gamma + 1)\rho^2 = \left(\frac{1}{2(1+\sigma^2)^2} + 1 \right) \rho^2 < 1 \quad \Leftrightarrow \quad \rho < \sqrt{\frac{2\sigma^4 + 4\sigma^2 + 2}{2\sigma^4 + 4\sigma^2 + 3}}.$$

In particular, for highly stochastic gradients, the decay rate ρ can be chosen close to 1. For less stochastic gradients, to achieve similar ρ , a more conservative choice of $\alpha\gamma$ is required. The decay factor

$$\eta - \alpha\gamma(1+\sigma^2) = \eta - \frac{\eta}{2} = \frac{1}{2L(1+\sigma^2)}$$

scales with the stochasticity σ of the gradient estimators and the Lipschitz constant L of the objective function.

Proof. Consider

$$\mathcal{L}_n = \mathbb{E} \left[f(x_n) + \frac{\lambda}{2} \|\alpha v_n\|^2 \right].$$

for a parameter $\lambda > 0$ to be fixed later. We have

$$\begin{aligned} \mathbb{E}[f(x_{n+1})] &\leq \mathbb{E}[f(x'_n)] - \frac{\eta}{2} \mathbb{E}[\|\nabla f(x'_n)\|^2] \\ &\leq \mathbb{E} \left[f(x_n) + \nabla f(x'_n) \cdot \alpha v_n + \frac{L\alpha^2}{2} \|v_n\|^2 - \frac{\eta}{2} \|\nabla f(x'_n)\|^2 \right] \\ \mathbb{E}[\|\alpha v_{n+1}\|^2] &= \rho^2 \mathbb{E}[\|\alpha v_n\|^2 - 2(\alpha\gamma) \alpha v_n \cdot g_n + (\alpha\gamma)^2 \|g_n\|^2] \end{aligned}$$

by Lemmas 14 and 17. We deduce that

$$\begin{aligned} \mathcal{L}_{n+1} &\leq \mathbb{E}[f(x_n)] + (1 - \lambda\alpha\gamma\rho^2) \mathbb{E}[\nabla f(x'_n) \cdot \alpha v_n] + \frac{L + \lambda\rho^2}{2} \|\alpha v_n\|^2 \\ &\quad + \frac{\lambda\rho^2\alpha\gamma \cdot \alpha\gamma(1+\sigma^2) - \eta}{2} \mathbb{E}[\|\nabla f(x'_n)\|^2] \\ &\leq \mathcal{L}_n + \frac{\lambda\rho^2\alpha\gamma \cdot \alpha\gamma(1+\sigma^2) - \eta}{2} \mathbb{E}[\|\nabla f(x'_n)\|^2] \end{aligned}$$

under the conditions

$$1 - \lambda\alpha\gamma\rho^2 = 0, \quad L + \lambda\rho^2 \leq \lambda.$$

The first condition implies that $\lambda = (\alpha\gamma\rho^2)^{-1}$, so the second one reduces to

$$(1 - \rho^2)\lambda = \frac{1 - \rho^2}{\rho^2\alpha\gamma} \geq L \quad \Leftrightarrow \quad 1 - \rho^2 \geq L\rho^2\alpha\gamma \quad \Leftrightarrow \quad 1 \geq (1 + L\alpha\gamma)\rho^2.$$

Finally, we consider the last equation. If

$$\varepsilon := \eta - \lambda\rho^2\alpha\gamma \cdot \alpha\gamma(1+\sigma^2) = \eta - \alpha\gamma(1+\sigma^2) > 0,$$

then we find that

$$\mathbb{E} \left[f(x_1) + \frac{1}{\alpha\gamma\rho^2} \|v_1\|^2 - \inf f \right] \geq \mathcal{L}_1 - \mathcal{L}_{n+1} = \sum_{i=1}^n (\mathcal{L}_i - \mathcal{L}_{i+1}) \geq \frac{\varepsilon}{2} \sum_{i=1}^n \mathbb{E}[\|\nabla f(x_i)\|^2]$$

and hence

$$\min_{1 \leq i \leq n} \mathbb{E}[\|\nabla f(x_i)\|^2] \leq \frac{1}{n} \sum_{i=1}^n \mathbb{E}[\|\nabla f(x_i)\|^2] \leq \frac{2\mathbb{E}[f(x_1) - \inf f + \frac{1}{\alpha\gamma\rho^2} \|v_1\|^2]}{\varepsilon n}.$$

□

APPENDIX H. PROOFS OF THEOREMS 4 AND 6: CONVEX OPTIMIZATION

We first recall the statement of the convergence result.

Theorem 4 (Convex case). *Assume that, in addition to the assumptions laid out in Section 3.3, the objective function f is convex and that x^* is a point such that $f(x^*) = \inf_{x \in \mathbb{R}^m} f(x)$. Assume that α, η, γ are parameters such that*

$$\eta = \frac{1}{L(1 + \sigma^2)}, \quad \gamma\alpha = \frac{\eta}{2(1 + \sigma^2)}, \quad n_0 \geq \sqrt{(2\sigma)^4 + 24\sigma^2 + 10} - 2, \quad \rho_n = \frac{n + n_0}{n + n_0 + 3}$$

and $\rho_n = \frac{n + n_0}{n + n_0 + 3}$. Then

$$\mathbb{E}[f(x_n) - f(x^*)] \leq \frac{\mathbb{E}[(n_0\gamma\alpha + 2\eta)n_0(f(x_0) - \inf f) + 2\|x_0 - x^*\|^2]}{\gamma\alpha(n + n_0)^2}.$$

Furthermore $f(x_n) \rightarrow \inf f$ with probability 1.

From the first order convexity condition

$$f(y) \geq f(x) + \nabla f(x) \cdot (y - x)$$

we deduce the more useful formulation $\nabla f(x) \cdot (x - y) \geq f(x) - f(y)$.

Proof. Set-up. Consider the Lyapunov sequence

$$\mathcal{L}_n = P(n) \mathbb{E}[f(x_n) - f(x^*)] + \frac{1}{2} \mathbb{E}[\|\alpha(n + n_0)v_n + 2(x'_n - x^*)\|^2]$$

where $P(n) = ((n + n_0)\gamma\alpha + 2\eta)(n + n_0)$. Over the course of a few steps, we will show that \mathcal{L}_n is decreasing in n .

Step 1. Let us consider the first term. Note that

$$\begin{aligned} \mathbb{E}[f(x_{n+1})] &= \mathbb{E}[f(x'_n - \eta g_n)] \\ &\leq \mathbb{E}[f(x'_n)] - c_{\eta, \sigma, L} \mathbb{E}[\|\nabla f(x'_n)\|^2] \end{aligned}$$

where $c_{\eta, \sigma, L} = \eta \left(1 - \frac{L\eta(1 + \sigma^2)}{2}\right) \leq \eta/2$ if $\eta \leq \frac{1}{L(1 + \sigma^2)}$.

Step 2. We now turn to the second term. First observe that

$$x'_{n+1} = x_{n+1} + \alpha v_{n+1} = x'_n - \eta g_n + \alpha v_{n+1}$$

and thus, if we denote $Z_n = \|(n + n_0)\alpha v_n + 2(x'_n - x^*)\|^2$, then

$$\begin{aligned} Z_{n+1} &= \|(n + n_0 + 1)\alpha v_{n+1} + 2(x'_n - \eta g_n + \alpha v_{n+1} - x^*)\|^2 \\ &= \|(n + n_0 + 3)\rho_n\alpha(v_n - \gamma g_n) + 2(x'_n - x^*) - 2\eta g_n\|^2 \\ &= \|(n + n_0)\alpha v_n + 2(x'_n - x^*) - ((n + n_0)\gamma\alpha + 2\eta)g_n\|^2 \end{aligned}$$

since $(n + n_0 + 3)\rho_n = n + n_0$. In particular

$$Z_{n+1} = Z_n - 2((n + n_0)\gamma\alpha + 2\eta) \langle g_n, (n + n_0)(x'_n - x_n) + 2(x'_n - x^*) \rangle + ((n + n_0)\gamma\alpha + 2\eta)^2 \|g_n\|^2.$$

Step 3. So far, we exploited L -smoothness in Step 1, but not convexity. We find that in expectation

$$\begin{aligned} \mathbb{E}[Z_{n+1}] &= \mathbb{E}[Z_n] - 2((n + n_0)\gamma\alpha + 2\eta) \mathbb{E}[g_n \cdot ((n + n_0)(x'_n - x_n) + 2(x'_n - x^*))] \\ &\quad + ((n + n_0)\gamma\alpha + 2\eta)^2 \mathbb{E}[\|g_n\|^2] \\ &\leq \mathbb{E}[Z_n] - 2((n + n_0)\gamma\alpha + 2\eta) \mathbb{E}[(n + n_0) \nabla f(x'_n) \cdot (x'_n - x_n) + 2 \nabla f(x'_n) \cdot (x'_n - x^*)] \\ &\quad + ((n + n_0)\gamma\alpha + 2\eta)^2 (1 + \sigma^2) \mathbb{E}[\|\nabla f(x'_n)\|^2] \\ &\leq \mathbb{E}[Z_n] - 2((n + n_0)\gamma\alpha + 2\eta) \mathbb{E}[(n + n_0)(f(x'_n) - f(x_n)) + 2(f(x'_n) - f(x^*))] \\ &\quad + ((n + n_0)\gamma\alpha + 2\eta)^2 (1 + \sigma^2) \mathbb{E}[\|\nabla f(x'_n)\|^2]. \end{aligned}$$

Step 4. Combining the estimates, we find that

$$\begin{aligned}
& \mathbb{E} \left[P(n+1) (f(x_{n+1}) - f(x^*)) + \frac{1}{2} \|(n+n_0+1)\alpha v_{n+1} + 2(x'_{n+1} - x^*)\|^2 \right] \\
& \leq P(n+1) \mathbb{E}[f(x'_n) - f(x^*)] - \frac{\eta P(n+1)}{2} \mathbb{E}[\|\nabla f(x'_n)\|^2] \\
& \quad + \frac{1}{2} \mathbb{E}[Z_n] - ((n+n_0)\gamma\alpha + 2\eta) \mathbb{E}[(n+n_0)(f(x'_n) - f(x_n)) + 2(f(x'_n) - f(x^*))] \\
& \quad + \frac{1}{2} ((n+n_0)\gamma\alpha + 2\eta)^2 (1 + \sigma^2) \mathbb{E}[\|\nabla f(x'_n)\|^2] \\
& = \mathbb{E} \left[P(n) (f(x_n) - f(x^*)) + \frac{1}{2} \|(n+n_0)\alpha v_n + 2(x'_n - x^*)\|^2 \right] \\
& \quad + P(n) \mathbb{E}[f(x'_n) - f(x_n)] + \{P(n+1) - P(n)\} \mathbb{E}[f(x'_n) - f(x^*)] \\
& \quad - ((n+n_0)\gamma\alpha + 2\eta)(n+n_0) \mathbb{E}[f(x'_n) - f(x_n)] - 2((n+n_0)\gamma\alpha + 2\eta) \mathbb{E}[f(x'_n) - f(x^*)] \\
& \quad + \left\{ \frac{1}{2} ((n+n_0)\gamma\alpha + 2\eta)^2 (1 + \sigma^2) - \frac{P(n+1)\eta}{2} \right\} \mathbb{E}[\|\nabla f(x'_n)\|^2] \\
& = \mathbb{E} \left[P(n) (f(x_n) - f(x^*)) + \frac{1}{2} \|(n+n_0)\alpha v_n + 2(x'_n - x^*)\|^2 \right] \\
& \quad + \{P(n) - ((n+n_0)\gamma\alpha + 2\eta)(n+n_0)\} \mathbb{E}[f(x'_n) - f(x_n)] \\
& \quad + \{P(n+1) - P(n) - 2((n+n_0)\gamma\alpha + 2\eta)\} \mathbb{E}[f(x'_n) - f(x^*)] \\
& \quad + \left\{ \frac{1}{2} ((n+n_0)\gamma\alpha + 2\eta)^2 (1 + \sigma^2) - \frac{P(n+1)\eta}{2} \right\} \mathbb{E}[\|\nabla f(x'_n)\|^2].
\end{aligned}$$

Step 5: First term. The equation is of the form

$$\mathcal{L}_{n+1} \leq \mathcal{L}_n + e_1 + e_2 + e_3.$$

It remains to choose the coefficients such that all error terms are non-positive. Since the first term $\mathbb{E}[f(x'_n) - f(x_n)]$ does not have an obvious sign, we selected the polynomial

$$P(n) = ((n+n_0)\gamma\alpha + 2\eta)(n+n_0)$$

to make sure that its coefficient vanishes. For the second and third term, it suffices to guarantee that the coefficients are non-positive.

Step 5: Second term. For the second error term, compute

$$\begin{aligned}
P(n+1) - P(n) &= ((n+n_0+1)\gamma\alpha + 2\eta)(n+n_0+1) - ((n+n_0)\gamma\alpha + 2\eta)(n+n_0) \\
&= (n+n_0)\gamma\alpha + 2\eta + \gamma\alpha(n+n_0) + \gamma\alpha \\
&= (2n+2n_0+1)\gamma\alpha + 2\eta
\end{aligned}$$

In particular, we find that the coefficient of the second term is non-positive if

$$(2n+2n_0+1)\gamma\alpha + 2\eta - 2((n+n_0)\gamma\alpha + 2\eta) = \gamma\alpha - 2\eta \leq 0.$$

We will see below that the third term requires a stricter condition on the size of $\gamma\alpha$ compared to η which will imply this one.

Step 5: Third term. Finally, consider the coefficient of the third term

$$((n+n_0)\gamma\alpha + 2\eta)^2 (1 + \sigma^2) - \eta P(n+1)$$

(up to a factor of 1/2). This term is negative if and only if

$$\begin{aligned}
(1 + \sigma^2) \{(\gamma\alpha)^2 (n+n_0)^2 + 4\eta\gamma\alpha(n+n_0) + 4\eta^2\} &\leq \eta\gamma\alpha(n+n_0+1)^2 + 2\eta^2(n+n_0+1) \\
&= \eta\gamma\alpha(n+n_0)^2 + 2(\eta^2 + \eta\gamma\alpha)(n+n_0) + 2\eta^2 + \eta\gamma\alpha
\end{aligned}$$

For easier readability, we denote $z := n + n_0$ and $R = \frac{\gamma\alpha}{\eta}$ such that $\eta = R\gamma\alpha$. The condition is equivalent to requiring that

$$\gamma\alpha\{(1 + \sigma^2)\gamma\alpha - \eta\}z^2 + \eta\{4\gamma\alpha(1 + \sigma^2) - 2\eta - 2\gamma\alpha\}z + 4\eta^2(1 + \sigma^2) - 2\eta^2 - \eta\gamma\alpha \leq 0.$$

If $R \geq \max\{2, 1 + \sigma^2\}$, we note that $2\eta \geq \eta \geq \gamma\alpha$ and that the coefficient of the quadratic term is non-positive. The expression simplifies as

$$\eta\gamma\alpha\left\{\left(\frac{1 + \sigma^2}{R} - 1\right)z^2 + (2(1 - R) + 4\sigma^2)z + (2R + 4R\sigma^2 - 1)\right\} \leq 0.$$

Specifically, we consider $R = 2(1 + \sigma^2)$, at which point the inequality reads

$$\begin{aligned} 0 &\geq -\frac{1}{2}z^2 + (2 - 4(1 + \sigma^2) + 4\sigma^2)z + (4(1 + \sigma^2) + 8\sigma^2(1 + \sigma^2) - 1) \\ &= -\frac{z^2}{2} - 2z + (8\sigma^4 + 12\sigma^2 + 3). \end{aligned}$$

The value we deduce for n_0 is therefore the larger of the two zeros of the quadratic polynomial $z^2 + 4z - (16\sigma^4 + 24\sigma^2 + 6)$:

$$n_0 = -\frac{4}{2} + \sqrt{\left(\frac{4}{2}\right)^2 + 16\sigma^4 + 24\sigma^2 + 6} = \sqrt{(2\sigma)^4 + 24\sigma^2 + 10} - 2$$

For different σ , the value of n_0 asymptotically as $(2\sigma)^2$. We furthermore observe that $n_0 \geq \sqrt{10} - 2 \approx 1.2$ for all values of $\sigma \geq 0$.

Step 6. Thus we have proved that \mathcal{L}_n is monotone decreasing in n if the coefficients are chosen as

$$\eta = \frac{1}{L(1 + \sigma^2)}, \quad \gamma\alpha = \frac{\eta}{2(1 + \sigma^2)}, \quad n_0 = \sqrt{(2\sigma)^4 + 24\sigma^2 + 10} - 2, \quad \rho_n = \frac{n + n_0}{n + n_0 + 3}$$

We have shown that, under suitable conditions on $\eta, \alpha\gamma$ and a particular choice of ρ_n , the estimate $\mathcal{L}_{n+1} \leq \mathcal{L}_n$ holds. We deduce that

$$\mathbb{E}[f(x_n) - f(x^*)] \leq \frac{\mathcal{L}_n}{P(n)} \leq \frac{\mathcal{L}_0}{P(n)} \leq \frac{\mathbb{E}[(n_0\gamma\alpha + 2\eta)n_0(f(x_0) - \inf f) + 2\|x_0 - x^*\|^2]}{\gamma\alpha(n + n_0)^2}.$$

Step 7. It remains to show that $f(x_n) \rightarrow f(x^*) = \inf f$ almost surely. This follows by standard arguments from the fact that the sequence of expectations $\mathbb{E}[f(x_n) - \inf f]$ is summable: By the previous argument, the estimate

$$\mathbb{E}[|f(x_n) - f(x^*)|] = \mathbb{E}[f(x_n) - f(x^*)] \leq \frac{C}{n^2}$$

holds for some $C > 0$. Since

$$\begin{aligned} \mathbb{P}\left(\lim_{n \rightarrow \infty} f(x_n) \neq \inf f\right) &= \mathbb{P}\left(\limsup_{n \rightarrow \infty} |f(x_n) - \inf f| > 0\right) \\ &= \mathbb{P}\left(\bigcup_{k=1}^{\infty} \left\{\limsup_{n \rightarrow \infty} |f(x_n) - \inf f| > \frac{1}{k}\right\}\right) \\ &\leq \sum_{k=1}^{\infty} \mathbb{P}\left(\limsup_{n \rightarrow \infty} |f(x_n) - \inf f| > \frac{1}{k}\right), \end{aligned}$$

it suffices to show that $\mathbb{P}(\limsup_{n \rightarrow \infty} |f(x_n) - \inf f| > \varepsilon) = 0$ for any $\varepsilon > 0$. We further note that for any $N \in \mathbb{N}$ we have

$$\begin{aligned} \mathbb{P}\left(\limsup_{n \rightarrow \infty} |f(x_n) - \inf f| > \varepsilon\right) &\leq \mathbb{P}(\exists n \geq N \text{ s.t. } |f(x_n) - \inf f| > \varepsilon) \\ &= \mathbb{P}\left(\bigcup_{n=N}^{\infty} \{|f(x_n) - \inf f| > \varepsilon\}\right) \\ &\leq \sum_{n=N}^{\infty} \mathbb{P}(|f(x_n) - \inf f| > \varepsilon) \\ &\leq \sum_{n=N}^{\infty} \frac{\mathbb{E}[|f(x_n) - \inf f|]}{\varepsilon} \\ &\leq \frac{C}{\varepsilon} \sum_{n=N}^{\infty} \frac{1}{n^2} \end{aligned}$$

by Markov's inequality. As the series over n^{-2} converges, the expression on the right can be made arbitrarily small by choosing N sufficiently large. Thus the quantity on the left must be zero, which concludes the proof. \square

Let us point out how the same techniques can be adapted to prove convergence $f(x_n) \rightarrow \inf f$, even if a global minimizer does not exist. We recall the main statement.

Theorem 6 (Convexity without minimizers). *Let f be a convex objective function satisfying the assumptions in Section 3.3. Assume that $\eta, \alpha, \gamma, n_0$ and ρ_n are as in Theorem 4. Then $\liminf_{n \rightarrow \infty} \mathbb{E}[f(x_n)] = \inf_{x \in \mathbb{R}^m} f(x)$.*

Proof. **Step 1.** The first step follows along the same lines as the proof of Theorem 4 with minor modifications. Note that we did not use the minimizing property of x^* except for Step 5.2. Assume for the moment that $\inf f > -\infty$.

Assume first that $\varepsilon := \liminf_{n \rightarrow \infty} \mathbb{E}[f(x_n)] - \inf f > 0$. Select x^* such that $f(x^*) < \inf f + \varepsilon/4$ and define the Lyapunov sequence \mathcal{L}_n just as in the proof of Theorem 4 with the selected point x^* .

We distinguish between two situations. First, assume that n satisfies $\mathbb{E}[f(x'_n)] \geq f(x^*)$. In this case we find that also $\mathbb{E}[f(x_{n+1})] \leq \mathbb{E}[f(x'_n)] \leq f(x^*)$.

On the other hand, assume that $\mathbb{E}[f(x'_n)] \geq f(x^*)$ for $n = 0, \dots, N$. In that case, the proof of Theorem 4 still applies, meaning that $\mathbb{E}[f(x_N)]$ cannot remain larger than $f(x^*) + \varepsilon/2$ indefinitely. In either case, we find that there exists $N \in \mathbb{N}$ such that $\mathbb{E}[f(x_N)] \leq f(x^*) + \varepsilon/2 < \liminf_{n \rightarrow \infty} \mathbb{E}[f(x_n)]$.

Note that the proof of Theorem 4 applies with $n' \geq n_0$ as a starting point and a non-zero initial velocity v_n . The argument therefore shows that, for every $n' \in \mathbb{N}$ there exists $N \in \mathbb{N}$ such that $\mathbb{E}[f(x_N)] \leq \liminf_{n \rightarrow \infty} \mathbb{E}[f(x_n)]$. Inserting the definition of the lower limit, we have reached a contradiction. \square

When following this strategy, the key question is how far away the point x^* must be chosen. For very flat functions such as

$$f_\alpha : \mathbb{R} \rightarrow \mathbb{R}, \quad f_\alpha(x) = \begin{cases} x^{-\alpha} & x > 1 \\ 1 + \alpha(1 - x) & x \leq 1, \end{cases}$$

x^* may be very far away from the initial point x_0 , and the rate of decay can be exorbitantly slow if minimizers do not exist. For an easy example, we turn to the continuous time model. The solution to the heavy ball ODE

$$\begin{cases} x'' = -\frac{3}{t} x' - f'_\alpha(x) & t > 1 \\ x = 1 & t = 1 \\ x' = -\beta & t = 1 \end{cases}$$

is given by

$$x(t) = \left(\frac{4(3+\alpha)}{\alpha(2+\alpha)^2} \right)^{\frac{2}{2+\alpha}} t^{\frac{2}{2+\alpha}}$$

for $\beta = \frac{2}{2+\alpha} \left(\frac{4(3+\alpha)}{\alpha(2+\alpha)^2} \right)^{\frac{2}{2+\alpha}} > 0$. Solving the ODE backwards in time, we find that it is the solution for a more standard initial condition at time $t = 0$. Ignoring the complicated constant factor, we see that

$$f_\alpha(x(t)) = x(t)^{-\alpha} \sim t^{-\frac{2\alpha}{2+\alpha}},$$

the decay rate can be as close to zero as desired for α close to zero. For comparison, the solution of the gradient flow equation

$$\begin{cases} z' = -f'_\alpha(z) & t > 0 \\ z = 1 & t = 0 \end{cases} \quad \text{is given by } z(t) = (1 + \alpha(2 + \alpha)t)^{\frac{1}{2+\alpha}} \Rightarrow f_\alpha(z(t)) \sim t^{-\frac{\alpha}{2+\alpha}}.$$

Thus, while both the heavy ball ODE and the gradient flow can be made arbitrarily slow in this setting, the heavy ball remains much faster.

KANAN GUPTA, DEPARTMENT OF MATHEMATICS, TEXAS A&M UNIVERSITY, 155 IRELAND STREET, COLLEGE STATION, TX 77840

Email address: `kanan@tamu.edu`

JONATHAN SIEGEL, DEPARTMENT OF MATHEMATICS, TEXAS A&M UNIVERSITY, 155 IRELAND STREET, COLLEGE STATION, TX 77840

Email address: `jwsiegel@tamu.edu`

STEPHAN WOJTOWYTSCH, DEPARTMENT OF MATHEMATICS, TEXAS A&M UNIVERSITY, 155 IRELAND STREET, COLLEGE STATION, TX 77840

Email address: `stephan@tamu.edu`